

Pittsburg State University

Pittsburg State University Digital Commons

Electronic Theses & Dissertations

Spring 5-12-2023

OPTIMIZING PROCESS CONDITIONS AND CHARACTERIZING ELASTOMERIC PROPERTIES OF IMMISCIBLE POLYMERS FOR 3D PRINTING APPLICATIONS

Matthew Long

Pittsburg State University, mlong@gus.pittstate.edu

Follow this and additional works at: <https://digitalcommons.pittstate.edu/etd>

 Part of the [Polymer Chemistry Commons](#)

Recommended Citation

Long, Matthew, "OPTIMIZING PROCESS CONDITIONS AND CHARACTERIZING ELASTOMERIC PROPERTIES OF IMMISCIBLE POLYMERS FOR 3D PRINTING APPLICATIONS" (2023). *Electronic Theses & Dissertations*. 450.

<https://digitalcommons.pittstate.edu/etd/450>

This Thesis is brought to you for free and open access by Pittsburg State University Digital Commons. It has been accepted for inclusion in Electronic Theses & Dissertations by an authorized administrator of Pittsburg State University Digital Commons. For more information, please contact digitalcommons@pittstate.edu.

OPTIMIZING PROCESS CONDITIONS AND CHARACTERIZING ELASTOMERIC
PROPERTIES OF IMMISCIBLE POLYMERS FOR 3D PRINTING APPLICATIONS

A Thesis Submitted to the Graduate School
in Partial Fulfillment of the Requirements
for the Degree of Master of Science

Matthew Long

Pittsburg State University

Pittsburg, Kansas

May, 2023

OPTIMIZING PROCESS CONDITIONS AND CHARACTERIZING ELASTOMERIC
PROPERTIES OF IMMISCIBLE POLYMERS FOR 3D PRINTING APPLICATIONS

Matthew Long

APPROVED:

Thesis Advisor

Dr. Jeanne H. Norton, The Department of Plastics Engineering Technology

Committee Member

Dr. Charles Neef, The Department of Chemistry

Committee Member

Mr. Paul Herring, The Department of Plastics Engineering Technology

ACKNOWLEDGEMENTS

Firstly, I would like to give my most sincere appreciation to my mentor and advisor, Dr. Jeanne H. Norton. Dr. Norton has been a foundational pillar throughout the entirety of my college education, including undergraduate and graduate studies. As my advisor, Dr. Norton has provided me with her knowledge and expertise, provided guidance and encouragement, given life advice, and been a great friend who I look up to dearly. Dr. Norton has provided me with the tools and confidence for the next step in my career and for that I am eternally grateful.

I would also like to acknowledge and thank my committee members: Dr. Charles Neef and Mr. Paul Herring for their advice and encouragement towards my research. I would like to thank the Department of Chemistry and the Polymer Chemistry Initiative for funding my position as a graduate research assistant. I am grateful for the faculty and staff, laboratory space, and equipment in the Kansas Polymer Research Center; and the Department of Plastics Engineering Technology at PSU. Everyone was always willing to provide advice and assistance.

I would also like to acknowledge Sebastian Henry, Joy Lee, Lukas Amershek, Carlos Palestino, Ely Parks, Kelsey Reeves, Garrett Schick, Katelyn Coble, Meg Norman, Gunner Mengarelli, Emma Springer, Garrett Burghart, Cole Cooper, Jason Holt, Kasey Reynolds, Tim Waisner, and Kristopher Light for their assistance with data acquisition and analysis.

Lastly, I would like to thank my parents, Terry and Lisa Berggren, for providing their unconditional love and support during this process. They have supported me and my decisions, whether it was financially, physically, or emotionally, and for that I am

grateful. I dedicate this thesis to those mentioned above because without these people, this would not have been possible. Thank you so much.

OPTIMIZING PROCESS CONDITIONS AND CHARACTERIZING ELASTOMERIC PROPERTIES OF IMMISCIBLE POLYMERS FOR 3D PRINTING APPLICATIONS

An Abstract of the Thesis by
Matthew Long

Within recent years, 3D printing within the plastics and polymer industries has become increasingly prevalent. Also known as additive manufacturing, 3D printing enables the creation of rapid prototypes for short production runs without the need for complex tooling. This allows for runs that are shorter and lower in cost than conventional processes. Polylactic acid (PLA) is a thermoplastic that is widely used in 3D printing for its mechanical properties and low cost. The qualities of PLA however are lacking in the areas of flexibility and toughness which is required in many prototyping scenarios. The solution to this is to incorporate TPU (thermoplastic polyurethane) within the matrix of PLA to address the issue with flexibility. There is another issue that arises with incorporating TPU within the PLA matrix. These materials are immiscible which poses a problem with creating filament within the needed specifications. The goal of this work was to blend PLA and TPU to create a 3D printer filament that exhibits the desirable properties from each material. An additional goal was to optimize the filament diameter to increase compatibility with the feed throat of the 3D printer, which allows for increased consistency of parts.

During the extrusion process, parameters such as screw speed, winder settings, and barrel temperatures were adjusted to try and create circular filament within the set specifications of 1.75 mm (+/- 0.05 mm). PLA and TPU blends were extruded at various ratios by weight percentage. Single-screw extrusion was performed on a Yellow Jacket

single-screw extruder in processing labs at Pittsburg State University. After processing, the filament was analyzed for its thermal, mechanical, and morphological properties. The methods used for thermal analysis were differential scanning calorimetry (DSC), thermogravimetric analysis (TGA), and melt flow index rheology. TGA was performed to determine degradation onset of the blends and DSC was performed to determine glass transition temperatures and melting temperatures of the crystalline fractions. Mechanical properties were analyzed via Instron tensile testing. Blends increasing in TPU percentage exhibited a change in strength and flexibility. Morphological analysis was performed via scanning electron microscopy (SEM). Furthermore, the transition between thermoplastic behavior and elastomeric behavior with increasing TPU incorporation was studied. In prior studies, glass transition temperatures and filament moduli shifted to values similar to TPU when the blend ratio was above 50% TPU. The filament was successfully produced and exhibited properties intermediate to PLA and TPU.

After filament was created successfully via single-screw extruder, filament blends were then created via twin-screw extrusion. This was done in order to determine if processing methods had a significant impact on filament blend properties. Various parameters, such as screw speed, hopper speed, zone temperatures, and winder speed were adjusted to achieve a filament within the desired specifications. Filament extruded via twin-screw extrusion was analyzed for thermal, mechanical, and morphological properties. Twin-screw filament was analyzed by the same thermal and mechanical methods as single-screw filament. The filament produced via twin-screw extrusion was within the specified diameter and was more dimensionally stable than filament produced by single-screw extrusion. Twin-screw extruded filament had less variation in melt

pressure than filament produced by single-screw extrusion. Thermal stability of filament blends was consistent regardless of processing methods. Mechanical analysis concluded that the modulus of twin-screw filament was slightly lower than single-screw filament. Melt flow index of pellets was significantly higher in single-screw extruded pellet than twin-screw extruded pellet.

Further work added an additional processing step: injection molding. Thermal, mechanical, and morphological analyses were also performed on specimens produced via injection molding. Injection-molded samples were analyzed by the same thermal and mechanical methods as single-screw and twin-screw filament. Impact testing was added, as we were able to produce impact bars in addition to tensile testing test bars in the injection molder. Future work involves 3D printing test bars using the filament produced by single-screw and twin-screw extrusion. Test bars would then be tested for tensile strength after printing and compared to injection-molded test bars.

TABLE OF CONTENTS

CHAPTER	PAGE
I. INTRODUCTION.....	1
1.1 Motivation.....	1
1.2 Polylactic Acid.....	2
1.3 Polyurethanes.....	4
1.3.1 Overview of Polyurethanes.....	4
1.3.2 Thermoplastic Polyurethanes.....	6
1.4 3D Printing.....	8
1.5 Material Compatibility Challenges.....	11
1.5.1 Immiscibility.....	11
1.5.2 Conventional Means of Overcoming Incompatibility.....	13
1.6 Extrusion Processing.....	15
1.6.1 Single-screw Extrusion.....	15
1.6.2 Twin-screw Extrusion.....	16
1.7 Injection Molding.....	19
1.8 Summary.....	21
II. OBJECTIVES.....	22
2.1 Overall Goals.....	22
2.2 Single-screw Extrusion of Immiscible Blends.....	22
2.3 Twin-screw Extrusion of Immiscible Blends.....	24
2.4 Injection Molding of Extruded Filament.....	24
2.5 Characterization of Starting Material, Filament, and Injection-Molded Parts.....	25
2.5.1 Determine and Compare Material Thermal Properties.....	25
2.5.2 Determine and Compare Material Mechanical Properties.....	26
2.5.3 Determine Blend Morphology.....	26
III. EXPERIMENTAL.....	27
3.1 Materials.....	27
3.1.1 Thermoplastic Materials.....	27
3.1.2 Solvents.....	28
3.2 Processing Methods.....	28
3.2.1 Material Drying.....	28
3.2.2 Extrusion Processing of Thermoplastic Materials.....	29
3.2.2.1 Single-screw Extrusion.....	29
3.2.2.1 Twin-screw Extrusion.....	30
3.2.3 Injection Processing of Thermoplastic Materials.....	32
3.3 Characterization Methods.....	33
3.3.1 Filament Diameter Measurement.....	33
3.3.2 Thermal Characterization.....	34
3.3.2.1 Thermogravimetric Analysis.....	34
3.3.2.2 Differential Scanning Calorimetry.....	34
3.3.2.3 Melt Flow Indexing.....	35
3.3.3 Mechanical Characterization.....	35
3.3.3.1 Tensile Testing.....	35
3.3.3.2 Izod Impact Testing.....	36
3.3.4 Characterization by Scanning Electron Microscopy.....	37
IV. RESULTS AND DISCUSSION – PLA PROCESSING INVESTIGATION AND SINGLE-SCREW EXTRUSION OF PLA/TPU BLENDS.....	38

4.1	PLA Processing Investigations.....	38
4.1.1	PLA Pellets Appearance.....	39
4.1.2	PLA Filament Appearance.....	39
4.1.3	Filament Diameter Measurements.....	40
4.1.4	PLA Test Bar Appearance.....	41
4.1.5	Thermogravimetric Analysis of PLA.....	41
4.1.6	Differential Scanning Calorimetry of PLA.....	43
4.1.7	Tensile Testing of PLA.....	44
4.1.8	Melt Flow Index Rheology of PLA.....	45
4.2	Single-screw Extrusion Processing of PLA/TPU Blends.....	46
4.2.1	Extruded Filament Appearance.....	46
4.2.2	Filament Diameter Measurements.....	48
4.2.3	Thermogravimetric Analysis of PLA/TPU Blends.....	50
4.2.4	Differential Scanning Calorimetry of PLA/TPU Blends.....	52
4.2.5	Tensile Testing of PLA/TPU Blends.....	54
4.2.6	SEM Characterization of PLA/TPU Blends.....	56
4.3	Summary.....	57
V.	RESULTS AND DISCUSSION – TWIN-SCREW EXTRUSION AND INJECTION MOLDING OF PLA/PTU BLENDS.....	60
5.1	Twin-screw Extrusion Processing.....	60
5.2	Appearance of PLA/TPU Pellets.....	61
5.3	Appearance of PLA/TPU Filaments.....	61
5.4	Filament Diameter Measurements.....	62
5.5	Thermogravimetric Analysis of Twin-screw Blends.....	63
5.6	Differential Scanning Calorimetry of Twin-screw Filament Blends.....	64
5.7	Melt Flow Indexing of Twin-screw Filament Blends.....	66
5.8	Tensile Testing of Twin-screw Filament Blends.....	67
5.9	SEM Characterization of Twin-Screw Blends.....	67
5.10	Injection Molding Processing of PLA/TPU Blends.....	68
5.11	Appearance of Injection-molded PLA/TPU Blends.....	69
5.12	Thermogravimetric Analysis of Injection-molded PLA/TPU Blends.....	69
5.13	Differential Scanning Calorimetry of Injection-molded PLA/TPU Blends.....	70
5.14	Tensile Testing of Injection-molded PLA/TPU Blends.....	72
5.15	Izod Impact Testing of Injection-molded PLA/TPU Blends.....	73
5.16	3D Printing with PLA Filament.....	74
5.17	Summary.....	74
VI.	CONCLUSIONS.....	77
6.1	Overview.....	77
6.2	PLA Processing.....	77
6.3	Single-screw Extrusion Versus Twin-screw Extrusion.....	79
6.4	Viability of Injection Molding PLA/TPU Blends.....	87
6.5	3D Printing.....	87
6.6	Future Work.....	88
6.7	Summary.....	88
	REFERENCES.....	91

LIST OF TABLES

TABLE	PAGE
Table 1. Drying Parameters for PLA and TPU.....	28
Table 2. Processing Parameters for Optimization for Single-screw Filament Blends.....	30
Table 3. Processing Parameters for Twin-screw Extrusion of PLA/TPU Blends.....	32
Table 4. Injection Molding Processing Parameters.....	33
Table 5. Filament Diameter Measurements of PLA Filaments.....	40
Table 6. TGA Data of PLA Produced by Varied Processes.....	42
Table 7. DSC Data of PLA Produced by Varied Processes.....	43
Table 8. Percent Crystallinity of PLA from Varied Processes.....	44
Table 9. Tensile Values of PLA Processed by Varied Methods.....	44
Table 10. Melt Flow Index of PLA through Different Processes.....	45
Table 11. Filament Diameter Measurements of Optimization Filaments.....	49
Table 12. Filament Diameter Measurements of Plastic-to-elastic Filaments.....	49
Table 13. Thermal Properties of PLA/TPU Optimization Blends.....	50
Table 14. Thermal Properties of PLA/TPU Plastic-to-elastic Blends.....	51
Table 15. DSC Values of Optimization Blends.....	53
Table 16. DSC Values of Plastic-to-elastic Blends.....	53
Table 17. Percent Crystallinity of Optimization Blends.....	53
Table 18. Percent Crystallinity of Plastic-to-elastic Blends.....	54
Table 19. Tensile Values of PLA/TPU Optimization Blends.....	55
Table 20. Tensile Values of PLA/TPU Plastic-to-elastic Blends.....	55
Table 21. Domain Size of TPU Domains in Optimized Filaments.....	56
Table 22. Domain Size of TPU Domains in Plastic-to-elastic Filaments.....	57
Table 23. Twin-screw Filament Diameter Measurements.....	62

Table 24. Thermal Properties as Determined by TGA of Twin-screw Filament Blends.....	64
Table 25. Thermal Properties as Determined by DSC for Twin-screw Filament Blends.....	64
Table 26. Percent Crystallinity of Twin-screw Filament Blends.....	65
Table 27. Melt Flow Index Values for Twin-screw Extrusion.....	66
Table 28. Tensile Modulus and Ultimate Elongation of Twin-screw Filament.....	67
Table 29. Domain Size of TPU Domains in Twin-screw Filaments.....	68
Table 30. Thermal Properties as Determined by TGA of Injection-molded Samples.....	70
Table 31. Thermal Properties as Determined by DSC of Injection-molded Samples.....	71
Table 32. Percent Crystallinity of Injection-molded Samples.....	72
Table 33. Tensile Modulus and Ultimate Elongation of Injection-molded Samples.....	72
Table 34. Izod Values of Injection-molded PLA/TPU Blends	73

LIST OF FIGURES

FIGURE	PAGE
Figure 1. Chemical structure of lactic acid monomer.....	2
Figure 2. Schematic representation of PLA synthesis	3
Figure 3. Reaction scheme for the synthesis of polyurethane through an addition reaction between a bifunctional isocyanate and polyol.....	5
Figure 4. Schematic overview of thermoplastic polyurethane.....	7
Figure 5. Schematic of a FDM 3D printer.....	9
Figure 6. Diagram of the “stair-stepping” effect common in FDM 3D printing.....	11
Figure 7. Different types of copolymers utilized in <i>ex situ</i> copolymerization. Left to right: di-block, tri-block, and graft copolymer.....	14
Figure 8. Rotation direction of counter-rotating (left) and co-rotating screws (right).....	17
Figure 9. Extrusion screws containing various screw elements used for twin-screw extrusion....	17
Figure 10. Schematic of injection molding machine.....	19
Figure 11. Schematic of a mold for injection molding.....	20
Figure 12. Poly(lactic acid), left; and general polyurethane structure, right.....	28
Figure 13. Chemical structure of dimethylformamide.....	28
Figure 14. Wayne Yellowjacket single-screw extruder (left), Brabender puller/winder (center), and water bath for filament cooling (right).....	29
Figure 15. Complete single-screw extrusion line.....	29
Figure 16. LabTech twin-screw extruder (left) and LabTech water bath (right).....	31
Figure 17. Labtech puller (left) and Berlyn material grinder (right).....	31
Figure 18. Twin-screw extrusion line.....	31
Figure 19. Arburg 320S 500-150 injection molder.....	32
Figure 20. Test bar mold within the Arburg.....	33
Figure 21. End view of the filament.....	34
Figure 22. Dimensions of a “dog bone” tensile test bar.....	36

Figure 23. Dimensions of Izod impact test specimen.....	37
Figure 24. Appearance of virgin, single-screw, and twin-screw PLA pellets.....	39
Figure 25. Appearance of single-screw and twin-screw PLA filament.....	40
Figure 26. Appearance of virgin, single-screw, and twin-screw PLA injection-molded samples.....	41
Figure 27. TGA thermograms of PLA through different processes. Virgin PLA pellet (—), Single-screw PLA filament (—), Single-screw PLA filament pellet (—), Twin-screw PLA Filament (—), Twin-screw PLA filament pellet (—), Virgin PLA test bar (—), 100:0 IJ (Single-screw) (—), and 100:0 IJ (Twin-screw) (—).....	42
Figure 28. Appearance of individual PLA/TPU Filaments – optimization.....	47
Figure 29. Appearance of individual PLA/TPU Filaments focusing on the plastic-to-elastic material transition.....	48
Figure 30. TGA thermograms of the PLA/TPU single-screw optimization blends. 100/0 (—), 90/10 (—), 70/30 (—), 50/50 (—), 30/70 (—), 10/90 (—), and 0/100 (—)	
Figure 36. TGA thermograms of the PLA/TPU single-screw plastic-to-elastic blends. 70/30 (—), 65/35 (—), 60/40 (—), 55/45 (—), 50/50 (—), 45/55 (—), 40/60 (—), 35/65 (—), and 30/70 (—).....	50
Figure 31. TGA thermograms of the PLA/TPU single-screw plastic-to-elastic blends. 70/30 (—), 65/35 (—), 60/40 (—), 55/45 (—), 50/50 (—), 45/55 (—), 40/60 (—), 35/65 (—), and 30/70 (—).....	51
Figure 32. The cool down and second heat curves for 70/30 filament.....	52
Figure 33. SEM micrographs of PLA/TPU optimized blends at approximately 6000x magnification.....	56
Figure 34. SEM micrographs of PLA/TPU plastic-to-elastic blends at approximately 6000x magnification.....	57
Figure 35. Appearance of 100/0, 90/10, 70/30, 50/50, 30/70, 10/90, and 0/100 twin-screw pellets.....	61
Figure 36. Appearance of 100/0, 90/10, 70/30, 50/50, 30/70, 10/90, and 0/100 twin-screw filament.....	62
Figure 37. TGA thermograms of twin-screw PLA/TPU filament blends: 100/0 (—), 90/10 (—), 70/30 (—), 50/50 (—), 30/70 (—), 10/90 (—), and 0/100 (—).....	63
Figure 38. SEM micrographs of twin-screw blends at approximately 6000x magnification.....	68
Figure 39. Appearance of virgin PLA, single-screw PLA, twin-screw PLA, twin-screw 70/30, twin-screw 30/70, and twin-screw 0/100 injection-molded test bars.....	69

Figure 40. TGA thermograms of injection-molded PLA/TPU test bars: 100/0 (virgin) (—), 100/0 (single-screw) (—), 100/0 (twin-screw) (—), 70/30 (—), 30/70 (—), and 0/100 (—).....70

Figure 41. Proposed 3D printed part design (left) and actual printed part made with 100/0 PLA filament processed by twin-screw extrusion (right).....74

LIST OF ABBREVIATIONS

- ABS – Acrylonitrile butadiene styrene
- °C – Degrees Celsius
- °C/min – Degrees Celsius per minute
- DMF – Dimethylformamide
- DSC – Differential scanning calorimetry
- FDM – Fused deposition modeling
- FFF – Fused filament fabrication
- Ft*lb/in – Foot*pound/inch
- g – Gram
- g/10 min – Grams per 10 minutes
- IJ – Injection-molded
- kg – Kilogram
- L:D – Length to diameter
- MFI – Melt flow index
- μm/m-K – Micrometer per meter Kelvin
- mm – Millimeters
- m/min – Meters per minute
- mL/min – Milliliters per minute
- mm/min – Millimeters per minute
- MPa – Megapascals
- PLA – Poly(lactic acid)
- psi_p – Pounds per square inch (plastic pressure)

RPM – Revolutions per minute

SEM– Scanning electron microscopy

SLA – Stereolithographic apparatus

T_c – Crystallization temperature

T_g – Glass transition temperature

TGA – Thermogravimetric analysis

T_m – Melting temperature

TPU – Thermoplastic polyurethane

wt – Weight

wt % - Weight percent

CHAPTER I

1. INTRODUCTION

1.1 Motivation

Plastic filament is defined as extruded plastic thread with a cylindrical profile and a consistent diameter. For manufacturing purposes, it is typically wrapped around a spool.¹ Plastic filament has many applications with the primary application being used in additive manufacturing, also known as 3D printing. Plastic filaments can be used as feedstock for other plastic processes or be used to manufacture items such as ropes, twine, and brushes.² In additive manufacturing, there are two standard filament dimensions that are utilized: 1.75 mm and 3.0 mm. Filament with a diameter of 1.75 mm is more commonly used due to rigidity of 3.0 mm filament. Filament with a diameter of 3.0 mm is less flexible, requires a greater degree of heating during printing, and has a decreased printing speed compared to 1.75 mm diameter filament.³

For 3D printing, the most common use for plastic filament is fused deposition modeling (FDM). FDM involves melting filament while simultaneously being extruded onto a build platform to produce a predetermined part.⁵ Many plastic variants are used for this method, but traditionally acrylonitrile butadiene styrene (ABS) and polylactic acid (PLA) are used in 3D printing.⁶ Polylactic acid (PLA) is a bio-based thermoplastic that is often used in 3D printing because of its high strength, but PLA lacks flexibility and

toughness. Thermoplastic polyurethane (TPU) is both flexible and tough, but has low modulus and strength. For these reasons, TPU is rarely used for 3D printing. By blending these resins, we can achieve materials that possess the optimal desired properties of each of the component polymers, while minimizing less desirable properties. The resulting filament will possess high strength and high toughness while retaining flexibility. This will allow for parts that were not previously 3D printable to be printed, tested, and utilized. Another reason that both the plastics industry and society at large are interested is that both PLA and TPU can be sourced from environmentally friendly materials, which makes them more sustainable compared to the petrochemically-based resins like ABS.⁷

1.2 Polylactic Acid

Polylactic acid is a thermoplastic polyester that is widely used in in the plastics and polymer industry. It has become increasingly popular due to being produced from renewable resources such as sugarcane, corn, and beets.⁸ PLA is a bio-sourced, bio-absorbable, bio-compostable, and bio-degradable polymer. PLA has one of the highest production capacities among commercially-available bioplastics.⁸ Because of the nature of its monomer, PLA is a more sustainable alternative to manufacturing plastics derived from petrochemical sources.⁹ Lactic acid is the building block for the synthesis of PLA (shown in Figure 1).

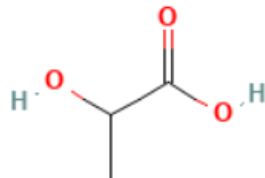


Figure 1. Chemical structure of lactic acid monomer.¹⁰

Bio-based PLA is synthesized in three steps: step 1: production of lactic acid by microbial fermentation; step 2: purification of lactic acid and preparation of its cyclic

dimer; and step 3: polycondensation of lactic acid or ring-opening polymerization of lactides. Figure 2 shows the reaction mechanism for both polycondensation of lactic acid and the ring-opening polymerization of lactides.⁹

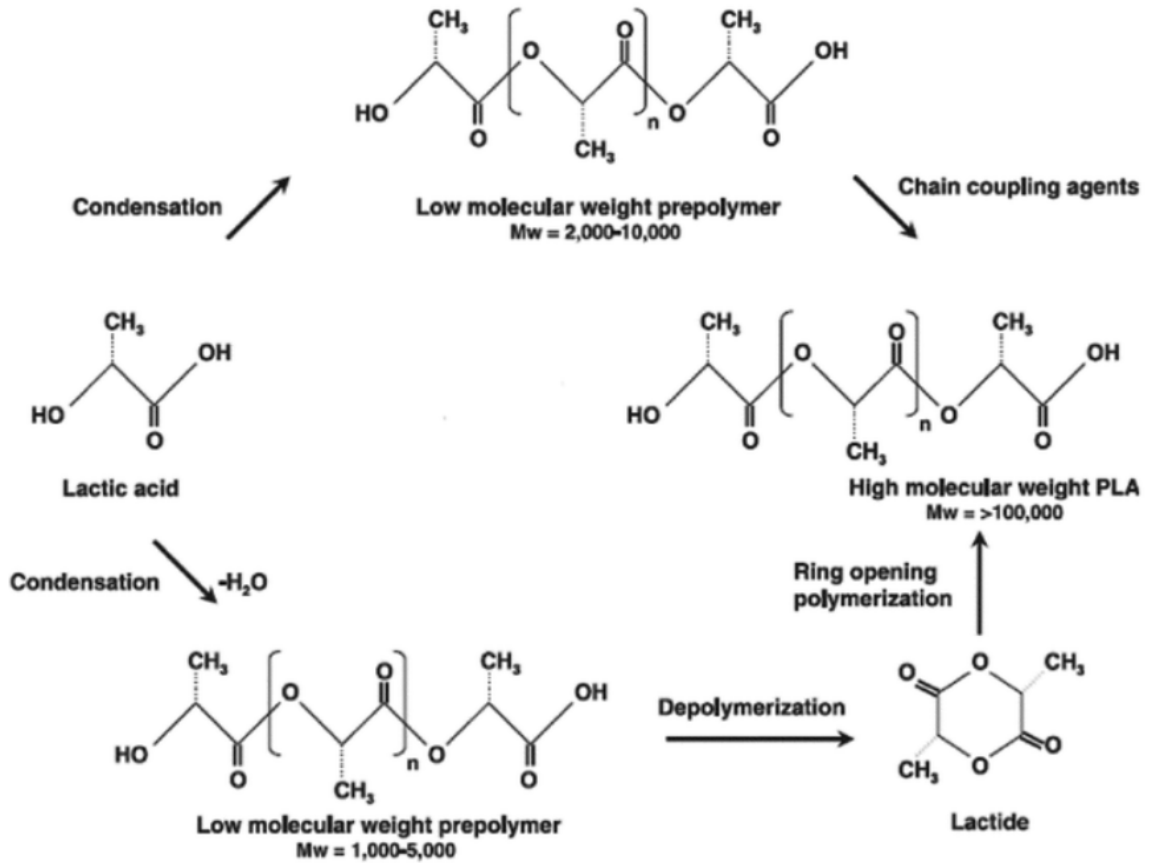


Figure 2. Schematic representation of PLA synthesis.⁹

PLA has many desirable properties that has made it the primary plastic filament material in 3D printing. It has a low melting range of 165-180 °C¹⁰ which makes it easily processible via 3D printing. PLA has a high tensile modulus of approximately 5800 MPa¹¹, which is superior to ABS which has a tensile modulus range of 1790 – 3200 MPa.¹² This allows for PLA to be used in applications that require a greater degree of mechanical strength than ABS can accommodate.⁷ PLA contains a low thermal expansion of 68 μm/m-K.¹² The thermal expansion range of ABS is 81-95 μm/m-K.¹² Lower thermal expansion indicates that PLA will have a greater level of dimensional stability

than ABS, and will produce a more desirable part.¹⁴ Lastly, PLA has superior layer adhesion compared to ABS. Layer adhesion issues can be caused by differences in temperature between the printed material and the print bed. A greater variation in temperature between the printed material and the print bed can lead to an increased amount of material warpage. Because PLA has a lower use temperature than that of ABS, it exhibits less issues with layer separation, and therefore, better interlayer adhesion.¹⁵ All these properties make PLA desirable for 3D printing when the end goal is a rigid, aesthetically pleasing part.⁷

1.3 Polyurethanes

1.3.1 Overview of Polyurethanes

Among polymers, polyurethanes are an increasingly versatile class of polymers which range in applications from insulators, foams, elastomers, coatings, and adhesives. Polyurethane chemistry first was developed through diisocyanate polyaddition reactions by Dr. Otto Bayer. Polyurethane chemistry reached industrial-scale synthesis in 1937. By the 1950's polyurethane chemistry had become established within the industrial market.¹⁶ Polyurethanes are characterized by the presence of a urethane linkage. They are able to be easily synthesized through an addition reaction between a difunctional alcohol and a difunctional isocyanate. The reaction scheme and general formula for a polyurethane is shown in figure 3.¹⁶

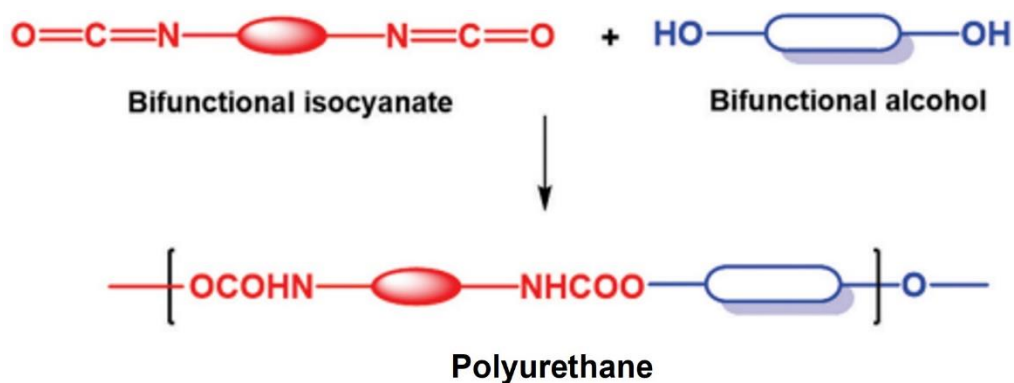


Figure 3. Reaction scheme for the synthesis of polyurethane through an addition reaction between a bifunctional isocyanate and polyol.¹⁶

Polyurethane chemistry is widely explored due to its straightforward synthesis. Modifications of the chemical structure of polyols or isocyanates are easily performed through various chemical approaches that allow polyurethane chemistry to have a wide range of properties. For example, an elastic polyurethane can be synthesized using polyol that contains a linear structure with high molecular weight but low functionality. Conversely, a rigid polyurethane can be synthesized by utilizing a polyol that contains aromatic groups in the structure as well as having a low molecular weight and higher functionality for crosslinking.¹⁶

Among industrial polymers, polyurethanes are among the materials with the fastest growing global market. The global polyurethane market was valued at over \$65 billion and is expected to increase at a rate of 3.2% until 2027.¹⁶ When used as an insulator, polyurethane foams exhibit positive economic and sustainable effects by decreasing energy consumption by 75% to 95%. Despite the increasing number of polyurethane applications, certain issues including flammability and sustainability still remain and merit scientific attention.¹⁶

1.3.2 Thermoplastic Polyurethanes

Polyurethane chemistry can be divided into two different categories: thermosets and thermoplastics. Thermosetting polyurethanes differ from thermoplastic polyurethanes in a few different ways. Thermosetting polyurethanes contain urethane linkages that are synthesized from multifunctional polyols and difunctional polyisocyanates. An average functionality greater than two across all reactants allows for crosslinking with results in a rigid 3D structure in thermosetting polyurethanes. Thermoplastic polyurethanes do not contain crosslinks unlike thermosetting polyurethanes. Thermoplastic polyurethanes are block copolymers made from rigid short-chain difunctional polyols and linear diisocyanates in “hard segment” chain-extending blocks combined with flexible, “soft segment” blocks from long-chain difunctional polyols and diisocyanates. The lack of crosslinking allows for increased flexibility and recyclability which is desirable in the additive manufacturing and rapid prototyping industry.¹⁷

Unlike thermosetting polyurethanes, thermoplastic polyurethanes are melt-processable thermoplastic elastomers with high durability and flexibility. TPU has a varying number of physical and chemical property combinations for many different applications including automotive parts, electrical coatings, films, textile coatings. Due to hard and soft segments, TPU exhibits properties between rigid plastic and flexible rubber. Because of its thermoplastic nature, it holds several benefits over traditional elastomers. It exhibits high mechanical strength comparative to other elastomers with a tensile modulus of 5 MPa.¹⁸ By comparison, polyolefin elastomers exhibit lower tensile strength with a tensile modulus ranging from 2-4 MPa.¹⁹ TPU also exhibits high flexibility with an ultimate elongation of 760%.¹⁸

Thermoplastic polyurethanes are typically produced through step-wise polyaddition reactions between a diisocyanate and one or more diols. The three basic raw materials required to produce TPU are a polyol or long-chain diol, a chain extender or short-chain diol, and a diisocyanate. This composition allows TPU to be a linear segmented block copolymer containing hard segments and soft segments. The soft segment is synthesized from an aliphatic difunctional polyol and diisocyanate. This section provides the flexibility and elastomeric character of TPU. The hard segment of TPU is constructed from a rigid aromatic short-chain diol chain-extender and diisocyanate, which provides the toughness and physical performance properties. The schematic overview of thermoplastic polyurethane is shown below.²⁰ The letter “P” in the schematic represents the polyol within the system. The letter “D” represents the diisocyanate within the system while the letter “C” the chain extender.

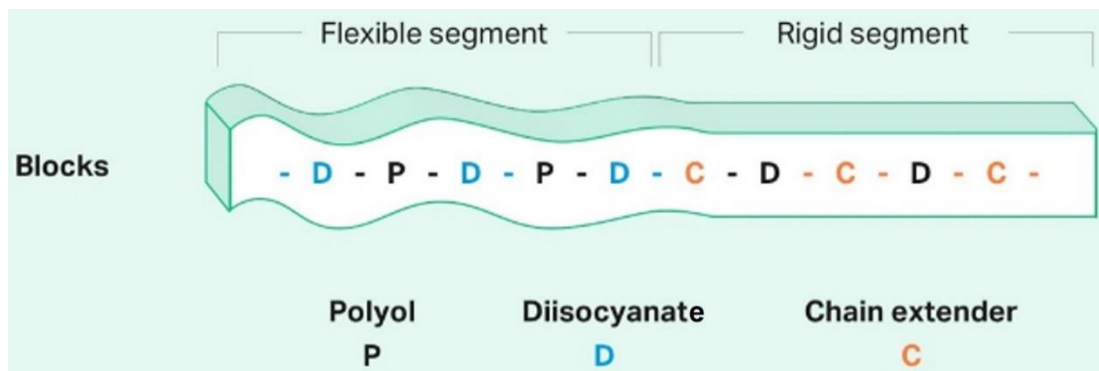


Figure 4. Schematic overview of thermoplastic polyurethane.²⁰

TPUs are highly tunable, and can be designed to meet different applications and processing methods. The non-ordered flexible segments of TPU are responsible for its resistance to chemicals, microbes, and hydrolysis. The characteristic of low-temperature flexibility can also be adjusted within the flexible segments. The rigid segments of TPU determine processing characteristics of TPU, like melting behavior and thermal

properties like degradation temperature. TPU Hardness can also be varied. Properties that are necessary for varied applications can be achieved by adjusting the composition of the hard and soft segments or by adjusting the ratio of soft and hard segments within the TPU.²⁰

1.4 3D Printing

In recent years, 3D printing has dramatically increased in prevalence within the plastics industry. The increased interest in 3D printing is due to the fact that 3D printing allows for short production runs or prototypes to be created very rapidly, inexpensively, and without complicated tooling. In addition, 3D printing allows for theories and hypotheses to be evaluated before expensive and/or time-intensive changes are made to materials, procedures, or equipment. Traditional prototyping involves producing and modifying a hardened steel mold which is a costly and time-intensive process. 3D printing can help avoid this step entirely.²¹

3D printing, also known as additive manufacturing, has existed in practice since the early 1970's when a patent for a process known as a "Liquid Metal Recorder" was submitted by Johannes F. Gottwald.²¹ This process envisioned a system that could produce an object made of liquified metal that solidified into a shape determined by system movement upon each new layer. This system used inkjet technology and paved the way for devices used for rapid prototyping that could move beyond ink including the process known as "material extrusion." In 1980, Dr. Hideo Kodama described two methods in a patent that used a thermosetting polymer instead of metal and laid the groundwork for modern additive manufacturing.²¹ Chuck Hull was the first person to successfully build a modern 3D printer. Based on Kodama's patent, Hull's design sent

special data from a digital file to the extruder of a 3D printer to build the object one layer at a time. In 1987, 3D Systems Corporation released the world's first stereolithographic apparatus (SLA) machine. SLA made it possible to manufacture complex parts, layer by layer, in a fraction of the time that normal manufacturing would require. This technology led to the invention of the .STL file that is still used to define part geometry in 3D printing today. The most common method for 3D printing was invented in 1989 by Scott Crump of Stratasys.²² This process, known as fused deposition modeling (FDM) or fused filament fabrication (FFF) involves molten thermoplastic filament extruded onto a print bed based on a predetermined design. A schematic of a FDM 3D printer is shown in Figure 5.²³

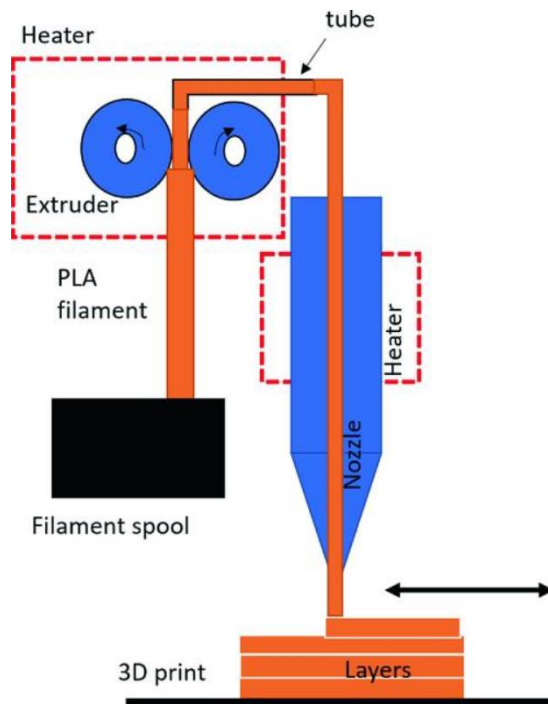


Figure 5. Schematic of a FDM 3D printer.²³

Pictured above is a schematic of a fused deposition modeling 3D printer. This technique utilizes plastics, in the form of filament, as the raw material or feedstock. The filament is cylindrical and is wound to a filament spool. To produce a part, filament is

continuously fed through the extruder and nozzle by the two rollers rotating in opposite directions. After passing through both heaters, molten plastic is deposited by the nozzle onto the printing platform layer-by-layer until the predetermined part is achieved. During this layering, the nozzle moves three-dimensionally per the spatial coordinates of the CAD model until the specified part is produced. Generally, the effectiveness and resolution of extrusion is highly dependent on the properties of the filament being extruded. Because of this, different FDM systems are designed for specific filament materials. Most low-cost FDM systems are only able to print with one type of thermoplastic material with PLA being the most common.²³

Utilizing PLA for FDM does not come without drawbacks. Compared to ABS, PLA has a higher degree of friction which makes it susceptible to extrusion blockages. Being a biopolymer, PLA degrades to natural and non-poisonous gases, when it is exposed to natural conditions, hydrolysis, or incineration. For these reasons, PLA is limited to certain applications.²³ PLA is often used in the medical field for stents and sutures due to biocompatibility.²⁴ PLA is also recognized by the Food and Drug Administration as food safe.²⁴

The process of FDM itself comes with drawbacks. FDM involves the continuous layering of molten plastic to create the predetermined product. The adhesion and fusion between adjacent layers are critical for quality prints. Accompanied with the extrusion conditions of the filament material during the printing process, this lack of layer adhesion can lead to surface roughness of printed products. This is known as the “stair-stepping” effect which is shown in figure 6.²³

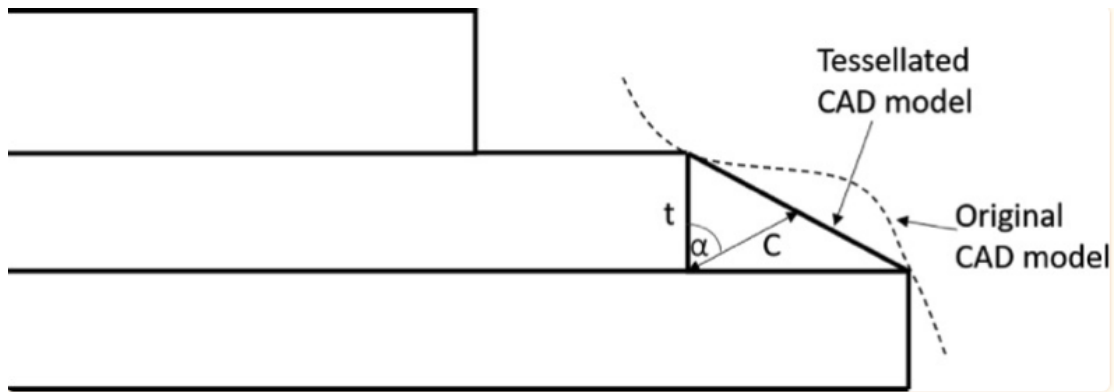


Figure 6. Diagram of the “stair-stepping” effect common in FDM 3D printing.²³

This effect is caused by the printing nozzle moving back and forth during the print process, which creates tracks. These tracks lead to terraces on the surface which lead to high levels of roughness values in the range of micrometers. Because of this, FDM is not used in dentistry or the biomedical field which require exceptional dimensional stability. These terraces can lead to the penetration of moisture between layers and attribute to further delamination issues. The “stair-stepping” effect may be unavoidable, but it can be minimized. Optimization of the print-slicing procedure and print resolution can attribute to a decrease in stair-stepping, but will increase print times which can hinder mass production by 3D printing. The flow rate of the material also has an effect on the print quality during FDM. It is crucial that extrusion temperatures are carefully chosen to avoid delamination. In this thesis, PLA is combined with TPU to potentially avoid this layer adhesion issue. PLA and TPU are immiscible, which poses its own issue to print quality.²⁵

1.5 Material Compatibility Challenges

1.5.1 Immiscibility

The polymers utilized in this research are immiscible with one another. Immiscibility is defined as where two substances are combined but unable to form a

stable homogeneous mixture. More specifically, it is indicative of an inability to mix on the molecular level.²⁶ When at rest, components of an immiscible mixture will separate from one another. One cause for separation is hydrophilic polar groups present within one mixture and hydrophobic non-polar groups present within the other. Density is another contributing factor to immiscibility. Less dense material rises to the top while more dense material will sink. This not only applies to liquids but also solids, and gases. In our case it applies to polymers in the melt. Immiscibility is often determined by optical methods. For a liquid, immiscibility can be determined in the bulk if liquids are stirred and the resulting mixture is cloudy. For a polymer blend, immiscibility can be determined via scanning electron microscopy.²⁷ SEM imaging can identify phase separation at the nanoscale within the system. Clear separation of polymer domains within a blend is indicative of complete or partial immiscibility in that blend. Miscible polymer blends rarely exhibit visible differences in domains when visualized in SEM.²⁸

Because PLA and TPU have differing polarity and hydrophilicity, they are immiscible in nature. PLA is hygroscopic in nature and contains a polar ester group. TPU used in this study is a segmented polymer consisting of hard urethane segments and soft polyester segments.²⁹ In a previous study involving this type of TPU, no hard segment melting was observed. Because of the lack of hard segment melting, it was concluded that the TPU was a co-polymer of different diols and perhaps different isocyanates.²⁹ With PLA and TPU, a certain degree of partial miscibility may be present. This is due to the hard segments of the urethane interacting with the amorphous regions of the PLA through hydrogen bonding to a greater extent than the soft segments of polyester. These materials have solubility parameters which are close to one another. These parameters being close

to each other allow for complete miscibility, but phase separation occurred due to entropic factors.²⁹

1.5.2 Conventional Means of Overcoming Incompatibility

Compounding is a process of blending polymers into formulations. It would be cost prohibitive to synthesize a new polymer for each application in which plastics are used. Compounding is a way to get a range of material properties with a relatively small number of polymer structures. Compounding improves material properties without requiring the synthesis of a unique polymer. It can improve mechanical properties, physical properties, thermal properties, and aesthetic properties.³⁰ This is accomplished by adding different small molecules to the polymer formulation during processing. Plasticizers, antioxidants, heat stabilizers, and slip agents are just a few examples of products added to polymers during production to improve certain properties. Plasticizers are added to polymer formulations to improve properties such as flexibility, durability, and flexibility of the polymer, while also reducing melt flow. Plasticizers function by reducing shear during the mixing steps of polymer production and improve impact resistance in the final plastic part. Antioxidants are embedded within various polymer resins to reduce the oxidative degradation of the polymer when exposed to ultraviolet light. Heat stabilizers are added to polymers to prevent thermal degradation of the polymer at elevated temperatures. Slip agents are added to polymers to reduce the surface coefficient of friction of a polymer. These additives provide lubrication to the film surface and also enhance the polymer with antistatic properties, enable better mold release, and reduce melt viscosity.

Compatibilizers are often utilized in the plastics industry when two incompatible polymeric materials are required in a formulation. Compatibilizers operate using three general principles: molecular diffusion at the interface allowing for polymer chains to become entangled, polar interactions between the two polymers, or chemical reactions between chemical groups in the polymers.³² There are three major methods to accomplish compatibilization of immiscible polymer blends: *ex situ* compatibilization, *in situ* compatibilization, and dynamic vulcanization. *Ex situ* compatibilization is a strategy which is developed using premade copolymers to improve compatibility between the blended components. This is a two-step process: synthesize copolymers that have suitable functionality; and melt blend the copolymer with an immiscible blend to improve component compatibility. Diblock, triblock, and graft copolymers are commonly used during *ex situ* copolymerization. These copolymers improve compatibility between two immiscible polymer blends by being miscible with each component of the immiscible polymer blend. Different types of copolymers that can be utilized for *ex situ* copolymerization are shown in figure 7.³³

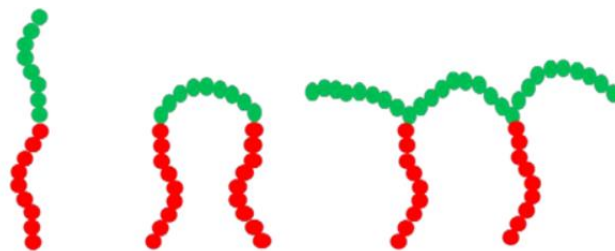


Figure 7. Different types of copolymers utilized in *ex situ* copolymerization. Left to right: di-block, tri-block, and graft copolymer.

In situ copolymerization is a strategy which utilizes polymers with reactive functional groups such as epoxies or isocyanates, to improve polymer blend compatibility. This method is successful with biodegradable polymers blends because these blends often contain reactive functional groups. During melt blending, the reactive

functional groups of the compatibilizer are capable of reacting with the functional groups of the blended components. This forms *in situ* graft and/or block copolymers. These newly formed copolymers act as compatibilizers within the blend system.

Dynamic vulcanization is the process of mixing a thermoplastic and rubber which is later cross-linked under dynamic conditions. In order to complete the vulcanization process, this is performed at high shear rates above the melting temperatures of both polymers.³³ While these methods are successful in overcoming incompatibility in polymer blends, a method suitable for industry production would want to by-pass these additives entirely. If complete or partial miscibility is able to be accomplished without additives, it would be more desirable to an industry partner to avoid this extra step.

Polymers can also be mechanically mixed, without the use of small molecules, to achieve desirable properties by blending. Blending is typically the most cost-effective method for improving polymer properties. Small molecule additives can greatly vary in price. Small molecule additives also can have a negative effect on the processing method used, especially if the molecule used is highly abrasive and is subject to high shearing forces. Small molecules can migrate out of the finished part, resulting in changes in part performance and potential part failure over time. Blending two thermoplastics can greatly improve the properties of the blend, without the potential downsides of utilizing small molecules. In general, blended plastics will have properties that are intermediate to the two plastics that were blended together.²⁹

1.6 Extrusion Processing

1.6.1 Single-screw Extrusion

The process of extrusion blends various stabilizers, additives, and fillers with various polymers or base resins to prepare specialized plastics formulations.³⁴ In this

study, two immiscible polymers will be blended through single-screw extrusion to achieve a desired formulation. The mechanical shearing of the polymers against the screw and extruder barrel allows for the even dispersion of one molten polymer in the presence of the other molten polymer to give the resulting blended material enhanced properties it did not have prior to compounding.³⁴ Single-screw extruders only contain one screw within the barrel which limits the mixing effect that the extruder has on a material blend. Extrusion screws are evaluated by their length to diameter ratio, or L:D ratio. The L:D ratio is the ratio of the length of the screw to the outside diameter of the screw. A common L:D ratio is 20:1, but longer ratios have been manufactured. Higher degrees of mixing can be achieved with larger L:D ratios that results in a more homogeneous mixture.³⁵

1.6.2 Twin-screw Extrusion

In this study, two immiscible polymers will also be blended through twin-screw extrusion to achieve a desired formulation. Twin-screw extrusion is a versatile and efficient process that accomplished higher degrees of mixing than single-screw extrusion. The mechanical shearing of the polymers against the screws and the extruder barrel allows for the even dispersion of one molten polymer in the presence of the other molten polymer to a much greater degree than in single-screw extrusion^{36,37} Twin-screw extrusion may employ one of two types of screw rotation which include counter-rotating and co-rotating screws. The direction of rotation for counter-rotating and co-rotating screws are shown in Figure 8.³⁸ Counter-rotating extruders achieve high-pressure buildup during processing as a result of the screws rotating in opposite directions. Co-rotating extruders achieve higher degrees of mixing during processing as a result of screws

rotating in the same direction. Twin-screw extrusion screws are also evaluated by their length to diameter ratio, or L:D ratio.³⁹

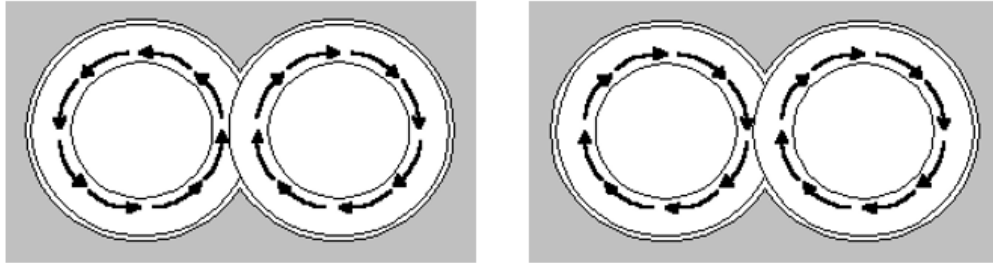
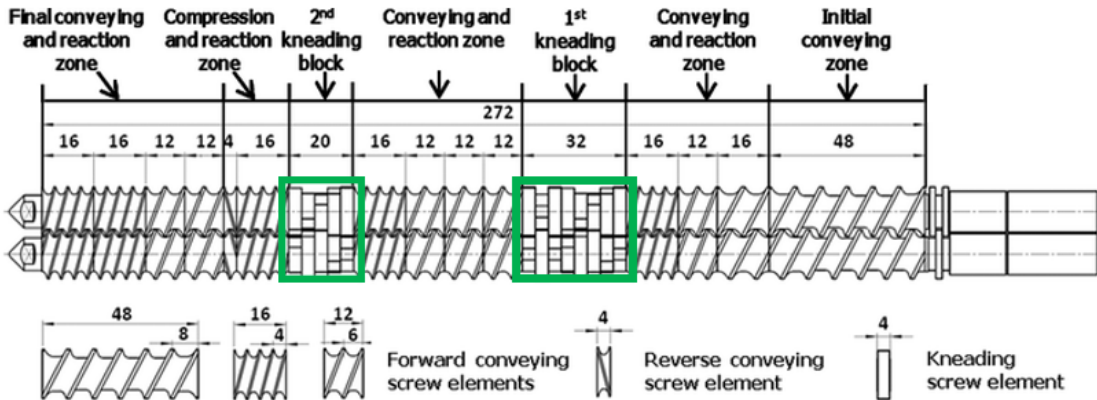


Figure 8. Rotation direction of counter-rotating (left) and co-rotating screws (right).³⁸

The screws of a twin-screw extruder contain different screw elements that are configurable to further improve mixing capability and achieve different properties in the blended extrudate.⁴⁰ Figure 9 displays the extrusion screws that contain various screw element used for twin-screw extrusion.⁴¹



Note: The mixing zones are boxed in green.

Figure 9. Extrusion screws containing various screw elements used for twin-screw extrusion.⁴¹

Numerous elements of the screw consist of kneading and conveying elements that are able to be incorporated into the screws to provide pressure build-up, elongation flow, shearing, and mixing to blend the plastic formulation. The screws can be divided into seven zones. The initial conveying zone, the conveying and reaction zone, the first

kneading block, an additional conveying and reaction zone, the second kneading block, the compression and reaction zone, and the final conveying and reaction zone.⁴¹

The initial conveying zone consists of conveying elements with the purpose of material transport from the hopper forward. The materials to be compounded are gravity fed from the hopper and conveyed forward from screw rotation in the initial conveying zone. The flights of the screws in this zone are generally the largest. This is for proper conveying of material. The channel depth of the screws is typically the same throughout the zone.⁴⁰ The material is transported from the initial conveying zone to the conveying and reaction zone. As this happens, channel depth and the screw flights of the barrel get progressively smaller. The mixing zones consist of various kneading elements or disks that are typically staggered at 30°, 45°, 60°, and 90° angles to produce high shearing stresses on the materials. This is to provide intensive mixing on the material. The kneading elements also contain small clearances between disks and between barrel surfaces. This is to further enhance mixing.

Depending on the screw design and configuration, the material will move through additional conveying and reaction zones as well as mixing zones. Toward the end of the extrusion process, the material moves to the compression and reaction zone. This zone consists of backward-conveying elements. These elements keep the material in the screw area for a longer amount of time with additional compression to provide a final opportunity for further mixing. The final conveying and reaction zone conveys the material to the end of the extruder and the material is guided through a die and exit the extruder.^{41,42}

1.7 Injection Molding

Injection molding is a common method for processing thermoplastic materials and is the largest sector of plastic processing. With injection molding, it is possible to accomplish high rates of production and low cycle times. Injection molding is able to cover a wide range of applications which allows for a variety of sizes and types of parts.⁴³ The components of an injection molder are shown in Figure 10.⁴⁴

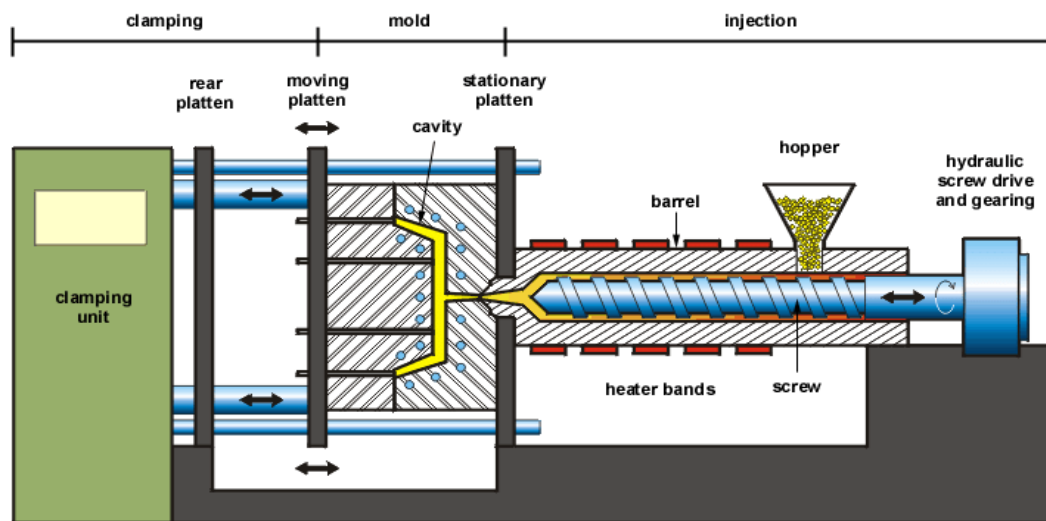


Figure 10. Schematic of injection molding machine.⁴⁴

Injection molding is a processing method to obtain molded products by injecting molten plastic material into a mold, followed by cooling and solidification of the plastic. Firstly, plastic pellets are fed into a hopper. Next, pellets are gravity-fed into the injection barrel. A rotating reciprocating screw melts and pushes the plastic through the barrel where it melts. As plastic pellets are melted and moved forward, the reciprocating screw moves backwards to build a pre-determined shot size. The shot size is the specified amount of material that will be injected from the barrel to the mold. As the reciprocating screw reaches the specified shot size, the screw is moved forward, injecting molten plastic through the nozzle of the barrel into a closed mold. Once the part is solidified, the

mold opens and ejects the part. A schematic of a mold for injection molding is shown in Figure 11.⁴⁵

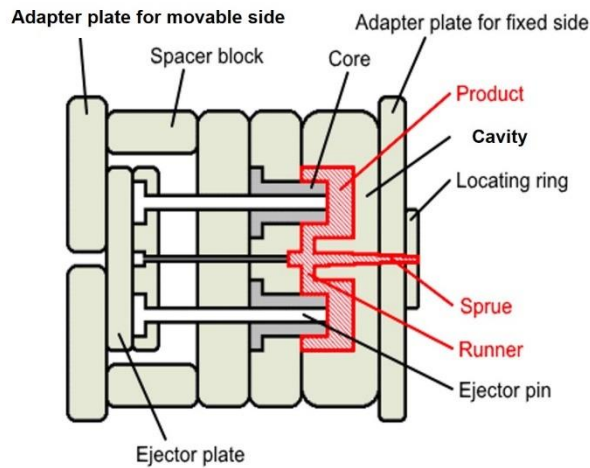


Figure 11. Schematic of a mold for injection molding.⁴⁵

A mold is a hollow block of metal, typically made of stainless steel. Many molds have holes drilled into them for temperature control. This temperature control can be accomplished by water, oil, or heaters. When molten plastic is injected into the mold, a sprue and runner system direct the molten plastic to the mold cavity to form the desired part shape. A mold may have multiple cavities to make more than one part in an injection molding cycle. When the molten resin is injected into the mold, it is contained inside the closed mold until it has solidified. The allotted amount of time set for the plastic to cool while inside the mold is known as the “cooling time.” As the molten plastic is cooling, the screw begins rotating again to build the shot for the next part. Once the cooling time is completed, the mold will open and eject the solidified part from the mold cavity by the ejector pins. The mold closes and repeats the process.⁴⁵

Because injection molding uses high amounts of pressure during each cycle, the mold is subject to high forces and requires a strong material to withstand that pressure. Mold tooling is typically costly not only due to material requirements, but the design

process that is required prior to mold fabrication. Mold design is an intricate process that requires high dimensional tolerances and finish. Additionally, the complexity of the design, size, and the expensive machines used to make the mold must be considered. After the process is up and running, additional costs will come from electricity, maintenance, accessory machines, and mold products.⁴⁶ Despite the high cost of tooling and machines, a successful injection molding line can be highly cost effective. The requirement of complex parts that require mass production is a primary reason why injection molding is cost effective. After initial production costs, injection molding would quickly produce thousands of the specified parts, in a fraction of time compared to 3D printing. 3D printing is cost effective through prototyping and short production runs. Anything relating to mass production, injection molding is highly superior.⁴⁷

1.8 Summary

The overall goal of this work is to successfully blend PLA with TPU to create a 3D printer filament that contains the strength of PLA and the flexibility and toughness of TPU. While working toward this goal, some challenges arose. First, since PLA and TPU are immiscible, it is imperative that the resins are mixed as well as possible. One possible route to addressing immiscibility was to change the morphological profile of the blends by adjusting processing parameters or blend ratios. In order for the filament to be viable for 3D printing, a cylindrical profile is most desirable and will result in fewer printing errors and better printed parts. Possible remedies were tested to remedy oblong filament including adjusting extrusion processing parameters and modifying the speed and traction of the pulley system that the filament passes through as it is wound onto a collection spool. Despite a few challenges that remain, the filament that was produced has met the specifications of our department's 3D printers in terms of shape and diameter.⁴⁸

CHAPTER II

2. OBJECTIVES

2.1 Overall Goals

The overall goal of this work was to determine if two immiscible polymers could be blended in order to achieve a material that exhibits the positive properties from each material while avoiding the less desirable properties. Specifically, we desire the strength of PLA with the enhanced flexibility of TPU. A secondary goal of the project was to investigate the effect of different processes on material properties. In order to determine this, multiple methods of processing were used including single-screw extrusion, twin-screw extrusion, and injection molding. Materials that were molded using these processes subsequently underwent thermal, mechanical, and optical characterization by thermogravimetric analysis (TGA), differential scanning calorimetry (DSC), Izod impact testing, tensile testing, melt flow index (MFI) testing, and scanning electron microscopy (SEM).

2.2 Single-screw Extrusion of Immiscible Blends

The effects of single-screw extrusion on two immiscible polymers using a commercial single-screw extruder were investigated. The single-screw extruder was used to extrude filament with varying ratios of PLA and TPU. Various blends of filament were successfully produced and subsequently analyzed. The optimal extrusion parameters for

all materials used in this work were determined. The molded materials included two controls (PLA and TPU) as well as blends of the two varying by weight percentage. For each material blend, filament was extruded with the intention that the filament would be within the designated specification of 1.75 mm (± 0.05). This specification is determined by the 3D printer, as viable filament that will successfully print will be within this specification. Processing conditions varied slightly for each resin blend. The procedure of determining the optimal processing conditions for each blend was as follows:

- Gather the control resin data sheets
- Prepare material blend ratios by weight
- Extrude the material blends
- Examine the filament for defects and adjust machine parameters accordingly
- Measure the resulting filament to determine cylindrical dimensions that are within specifications

The methods of analysis used for single-screw extruded filament were as follows: TGA, DSC, tensile testing, and SEM.

Once PLA/TPU blends were analyzed, it was discovered that material behavior shifted from classically plastic behavior to classically elastic behavior when the blend consisted of at least 70 wt% TPU. The plastic-to-elastic transition in the filament is characterized by a sharp change in specific material properties. In DSC, it is characterized by a significant shift to lower blend glass transition temperature. In tensile testing, it is characterized by a sharp decrease in filament modulus. The plastic-to-elastic

transition was more thoroughly explored by adjusting material blend ratios stepwise by five weight percent within the transition region.

2.2 Twin-screw Extrusion of Immiscible Blends

Twin-screw extrusion is favored over single-screw extrusion when blending and compounding. Twin-screw extrusion provides a greater level of mechanical mixing, even without the use of compatibilizers, compared to single-screw extrusion. This is primarily accomplished by the action of the two screws in the twin-screw extruder as opposed to only one in a single-screw extruder. The effects of twin-screw extrusion on two immiscible polymers using a commercial twin-screw extruder were then investigated. The twin-screw extruder was used to extrude filament with varying ratios of PLA and TPU that were similar to those processed in the single-screw extruder. Filament blends were successfully produced and subsequently analyzed. The procedure of determining the optimal processing conditions for each blend was similar to that of single-screw extruded filament described above. The methods of analysis used for twin-screw extruded filament were TGA, DSC, tensile testing, and SEM. Filament produced by method of twin-screw extrusion was superior in multiple areas compared to filament produced by method of single-screw extrusion. The primary area where filament is favored by twin-screw extrusion is dimensional stability.

2.3 Injection Molding of Extruded Filament

Plastics are typically injection-molded due to low operating cost and high efficiency compared to processing methods like extrusion. The first processing performed with injection molding was with various generations of PLA to identify if processing and regrinding subsequent generations influenced material properties. After this was

performed, various blends of PLA and TPU were injection-molded into test bars and subjected to analysis.

The optimal injection molding parameters for all materials used in this work were determined. The molded materials included two controls (PLA and TPU) as well as the blends of the two varying by weight percentage. All material was molded on the Arburg 320S Allrounder injection molder. For each material blend, two different types of test bars were molded to allow for further characterization. For each material, the settings on the Arburg were adjusted slightly to compensate for differing material properties. The parameters that differed were melt temperature, hold time, and cooling time. Shot size remained unchanged. Determining process parameters was a crucial step in receiving data that was accurate. Determining the optimal process conditions for each blend was similar to those of extrusion with the additional concern of examining initial parts for defects and adjusting process parameters, if needed. Methods of analysis used for injection-molded test bars were TGA, DSC, tensile testing, and Izod impact testing.

2.4 Characterization of Starting Material, Filament, and Injection-molded Parts

2.4.1 Determine and Compare Material Thermal Properties

Each control resin starting material was thermally characterized prior to melt processing as well as after extrusion or injection molding processing. The starting material pellets, filament, and molded material were subjected to TGA and DSC analysis. Pre-processed and post-processed samples were analyzed to determine if extrusion processing and/or injection molding had a significant effect on thermal, mechanical, and morphological properties. Materials were compared before and after processing to determine if material degradation had occurred. TGA was utilized to determine

degradation temperature, rate of degradation, and percent residue. DSC provided information about glass transition temperature (T_g), crystallization temperature (T_c), melting temperature (T_m), and percent crystallinity.

2.4.2 Determine and Compare Material Mechanical Properties

In order for mechanical properties to be evaluated, two different mechanical tests were performed on extruded filament and injection-molded samples: tensile testing and Izod impact testing. During tensile testing, a pulling force is applied to the material and the specimen's response to stress is determined. Tensile tests were performed on extruded filament specimens as well as injection-molded dog bone specimens. This test method was varied based on specimen dimensions as well as the analysis pull rate. Samples containing an increased amount of TPU took longer to measure due to increasing amounts of material flexibility compared to PLA samples.

Izod impact testing was performed on injection-molded samples. This method of characterization allowed for the material toughness to be studied. The impact strength of a material is determined by the loss of energy of the pendulum. Both notched and un-notched samples were analyzed for break type and impact strength. Varying blend ratios also affected Izod impact testing.

2.4.3 Determine Blend Morphology

In order for blend morphology to be evaluated, scanning electron microscopy (SEM) was performed on filament blends. SEM analysis was performed to determine the degree of nanoscale blending of immiscible polymers based on different processing methods. Images of the filament fracture surfaces were acquired at varying magnifications to visualize the distribution of TPU within the PLA matrices.

CHAPTER III

3. EXPERIMENTAL

3.1 Materials

3.1.1 Thermoplastic Materials

The project utilized two different thermoplastic materials which are immiscible. One behaves mechanically and thermally as a plastic and the other behaves as an elastomer. The reasoning for using materials that behave differently is to create a blended material that exhibits advantageous properties from both while minimizing the drawbacks that the pure individual materials display. The bioplastic that was used was Ingeo Biopolymer 3D870 homopolymer poly(lactic acid) (Natureworks, Blair, Nebraska, USA). This thermoplastic will be referred to as “PLA” from this point forward. PLA is a popular filament in 3D printing applications for its typically plastic behavior: a relatively high modulus with a yield point, indicating a tendency to be mechanically hard and strong, but brittle.

The elastomer that was used was Elastollan C60A10WH US thermoplastic polyurethane (TPU) (BASF, Florham Park, New Jersey, USA). This thermoplastic will be referred to as “TPU” from this point forward. TPU is a highly flexible elastomer, and is much less widely used for 3D printing compared to PLA. TPU exhibits typically elastic

behavior: a relatively low modulus with much higher elongation than PLA. The basic structure of PLA and polyurethane are shown in Figure 12.

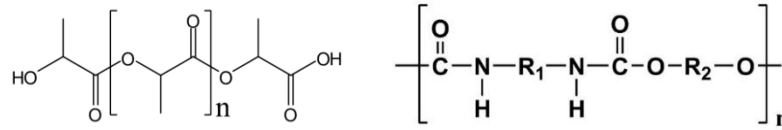


Figure 12. Poly(lactic acid), left; and general polyurethane structure, right.

3.1.2 Solvents

Dimethylformamide (DMF) was a solvent utilized for the treatment etching of various filament blends prior to SEM optical analysis. The structure of DMF is shown in Figure 13. TPU is soluble in DMF, while PLA is not. Samples soaked in DMF demonstrated the distribution of TPU within the PLA matrix for the purpose of visualizing TPU domain distribution by scanning electron microscopy.

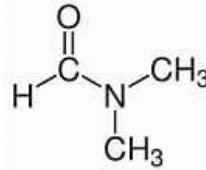


Figure 13. Chemical structure of dimethylformamide.

3.2 Processing Methods

3.2.1. Material Drying

Due to the hygroscopic nature of the materials utilized, each material required drying prior to further processing. Materials were dried overnight. The materials, trade name, drying temperature, minimum drying time, and actual drying time are reported in Table 1 below.

Table 1. Drying Parameters of PLA and TPU

Material	Trade Name	Drying Temperature (°C)	Minimum Drying Time (hours)	Actual Drying Time (hours)
PLA	Ingeo Biopolymer 3D870	49	8	16
TPU	Elastollan C60A10WH US	100	4	16

3.2.2 Extrusion Processing of Thermoplastic Materials

Initial process parameters for each process method described below were determined from each material data sheet. Process parameters were then adjusted based on the amount of PLA/TPU in each blend as needed to successfully process the materials.

3.2.2.1 Single-screw Extrusion

The Wayne Yellowjacket (Wayne Machine & Die Co., Totowa, New Jersey), shown in Figure 14, single-screw extruder was used for melt processing of various filament blends. Figure 14 also shows the Brabender puller/winder, used for the winding of filament blends after processing. (Brabender® GmbH & Co. KG, Duisburg, Germany), and the water bath used for cooling filament blends after they leave the single-screw extruder. The entire single-screw extrusion line is shown in figure 15. Table 2 details the optimized process parameters for all filaments processed by single-screw extrusion on the Yellowjacket extruder.



Figure 14. Wayne Yellowjacket single-screw extruder (left), Brabender puller/winder (center), and water bath for filament cooling (right).



Figure 15. Complete single-screw extrusion line.

Table 2. Processing Parameters for Optimization of Single-screw Filament Blends

Formulation (%PLA/%TPU)	Die Zone 2 (°C)	Die Zone 1 (°C)	Zone 3 (°C)	Zone 2 (°C)	Zone 1 (°C)	Screw Speed (RPM)	Take Off Speed (m/min)	Traction (%)
100/0	196.1	196.1	190.6	185	179	30	6.6	5
90/10	193.3	193.3	187.8	182.2	176.7	30	7	11
70/30	193.3	193.3	187.8	182.2	176.7	30	7	11
65/35	193.3	193.3	187.8	182.2	176.7	30	7.1	8
60/40	193.3	193.3	187.8	182.2	176.7	30	6.5	10.2
55/45	193.3	193.3	187.8	182.2	176.7	30	6.5	7.5
50/50	193.3	193.3	187.8	182.2	176.7	30	6	10
45/55	193.3	193.3	187.8	182.2	176.7	30	5	10
40/60	193.3	193.3	187.8	182.2	176.7	30	5	10
35/65	193.3	193.3	187.8	182.2	176.7	30	5	10
30/70	193.3	193.3	187.8	182.2	176.7	30	6	12
10/90	193.3	193.3	187.8	182.2	176.7	30	7	12
0/100	190.6	190.6	185	179.4	173.9	30	4.8	7

3.2.2.2 Twin-screw Extrusion

The LabTech twin-screw extruder 16mm twin-screw table top extruder (MiLabtech, LLC, Fenton, Michigan), shown in Figure 16 was used for melt processing of various filament blends. Figure 16 also shows the LabTech water bath (MiLabtech, LLC, Fenton, Michigan), used for the cooling of extruded filament after leaving the twin-screw extruder. Figure 17 shows the LabTech puller, (MiLabtech, LLC, Fenton, Michigan) used to pull and hold tension on twin-screw filament during processing. Figure 17 also shows the Berlyn material grinder (Worcester, MA) used for pelletizing. Figure 18 shows the twin-screw extrusion line. Table 3 details the optimized process parameters for all filaments processed by twin-screw extrusion on the Labtech extruder.



Figure 16. LabTech twin-screw extruder (left) and LabTech water bath (right).



Figure 17. Labtech puller (left) and Berlyn material grinder (right).



Figure 18. Twin-screw extrusion line.

Table 3. Processing Parameters for Twin-screw Extrusion of PLA/TPU Blends

Formulation (%PLA/%TPU)	Zones 1 - 10 (°C)	Screw Speed (RPM)	Hopper Speed (RPM)	Takeoff Speed (m/min)	Traction (%)
100/0	176.6	30	10	5	12
90/10	176.6	25	10	6	12
70/30	176.6	25	10	6	12
50/50	176.6	25	10	6	12
30/70	176.6	25	10	5	12
10/90	176.6	25	10	5	12
0/100	176.6	25	10	5	12

3.2.3. Injection Processing of Thermoplastic Materials

The Arburg Allrounder Injection Molding Machine, Model 320S 500-150 (Stammhaus Lossburg, Germany) was used for melt processing of PLA, TPU, and polymer blends. Shown in Figure 19, the Arburg has a clamping capacity of 55 tons and a screw diameter of 25mm. The maximum injection pressure is 36,259 psi_p. The intensification ratio is 18.2:1. Tie bar spacing is 320 mm x 320 mm. Opening stroke is 350 mm (hydraulic). Mold height (stack) minimum is 225 mm and 575 mm maximum. The knockout pattern is center and 7" x 7". Ejector stroke is 124 mm.⁴⁹



Figure 19. Arburg 320S 500-150 injection molder.

The Arburg was used to injection mold all material blends. Two types of test bars were molded according to standards ASTM D256 and ASTM D638 for the purpose of

mechanical testing.^{50,51} The test bar mold is shown in figure 20. Table 4 shows the processing parameters used for injection molding on the Arburg.



Figure 20. Test bar mold within the Arburg.

Table 4. Injection Molding Processing Parameters

Formulation (%PLA/%TPU)	Zones 1 - 5 (°C)	Mold Temperature (°C)	Shot Size (in)	Injection Speed (in/sec)	Hold Pressure (psi)	Hold Time (sec)	Cool Time (sec)
100/0	204	38	2.5	2	6000	10	30
70/30	204	38	2.5	2	6000	10	30
30/70	204	38	2.5	2	6000	10	30
0/100	226	38	3	2	5000	8	40

3.3 Characterization Methods

3.3.1 Filament Diameter Measurement

After extrusion, filament blend diameters were measured at two different points for each filament blend: 0° filament orientation and 90° filament orientation. Figure 21 details where these measurements were taken. Filament was measured every six feet. Measurements were recorded and averaged for each blend. The standard deviation of the 0° filament orientation and 90° filament orientation measurements was also calculated.

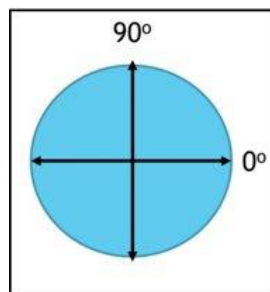


Figure 21. End view of the filament. Filament was measured at 0° filament orientation and 90° filament orientation to determine how cylindrical the final filament geometry was.

3.3.2 Thermal Characterization

3.3.2.1 Thermogravimetric Analysis

TGA was performed on resin pellets prior to molding and on all extruded filament samples. TGA was used to determine degradation behavior of each blend as well as percent residue (TA Instruments Thermogravimetric Analyzer, Model Q50, New Castle, Delaware, United States). All experiments were purged with nitrogen gas (60 mL/min purge flow rate) at a heating rate of 10 °C/min to 600 °C. Sample weights ranged from 5-10 milligrams. The temperatures at 10% and 50% weight loss, as well as percent residue, were recorded by TA Trios software.

3.3.2.2 Differential Scanning Calorimetry

DSC was performed on resin pellets prior to molding and on all extruded filament samples. DSC was used to determine the T_g , T_m , T_c , and percent crystallinity of each blend (TA Instruments Differential Scanning Calorimeter, Model Q100, New Castle, Delaware, United States). The material was first equilibrated to -80 °C. The first heating cycle was used to erase any prior thermal history of the materials at a heating rate of 10 °C/min to 250 °C. The materials were then cooled at a rate of 10 °C/min to -80 °C. The second heating cycle used a heating rate of 10 °C/min to 250 °C. The T_g , T_m , and T_c for each material was recorded by TA Universal Analysis software and TA Trios.

3.3.2.3 Melt Flow Indexing

A melt flow index (MFI) rheometer CEAST MF30 modular melt flow line, (Norwood, Massachusetts, USA) was used to determine the rheological properties of each polymer. Recorded in g/10 min, melt flow indexing was used to determine how quickly material flows in the melt using a specified temperature under a specified load. Melt flow was measured following ASTM D1238.⁵² For each resin, approximately 6 g of material was tested. A 2.16 kg load cell was used. The CeastVIEW 4.60 08 software generated a graph displaying melt flow rate (MFR) (g/10 min) as a function of time in seconds and calculated the MRF mean and MFR standard deviation values. The samples were analyzed at 210 °C, for a total of three runs per formulation. Average MFI and standard deviation were reported.

3.3.3 Mechanical Characterization

3.3.3.1 Tensile Testing

Tensile testing was used to determine the mechanical properties of filament blends and injection-molded dog bones. Figure 22 shows a diagram of dog bone sample measurements. An Instron 3367 tensile tester (Norwood, Massachusetts, USA) was used to perform the testing. The tensile procedure was determined based on the ASTM D638 procedure⁵¹ with varied pull rates based on the ratio of PLA/TPU in the blend. The dimensions of our test bars were: 165 mm by 19 mm by 3.2 mm with a gauge length of 13 mm.

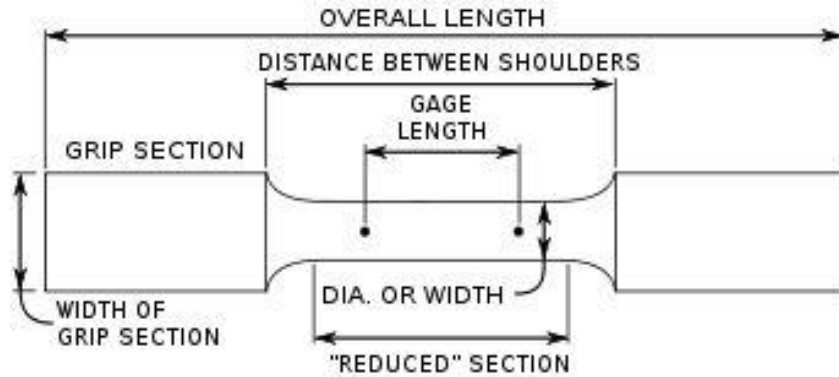


Figure 22: Dimensions of a “dog bone” tensile test bar.⁵³

3.3.3.2 Izod Impact testing

Izod impact testing was used to determine and compare the mechanical properties for each molded resin by using a Testing Machines Inc. (Islandia, New York, United States)⁵⁶ TMI 43-02-01 Monitor Impact Tester. The mechanical properties for each resin were determined according to the ASTM D256 10e1 procedure.⁵⁵ Ten injection-molded Izod test bars were cut in half to reflect the appropriate geometry for testing. Ten specimens were notched and subsequently tested. The other ten specimens were tested without modification (unnotched). The Izod test bars (63.5 mm long, 3.2 mm thick, and 12.7 mm wide) from each resin were analyzed at room temperature. Figure 23 displays the dimensions of the Izod test bar. The impact strength (Ft*lb/in) and break type from the notched and non-notched tests were recorded.

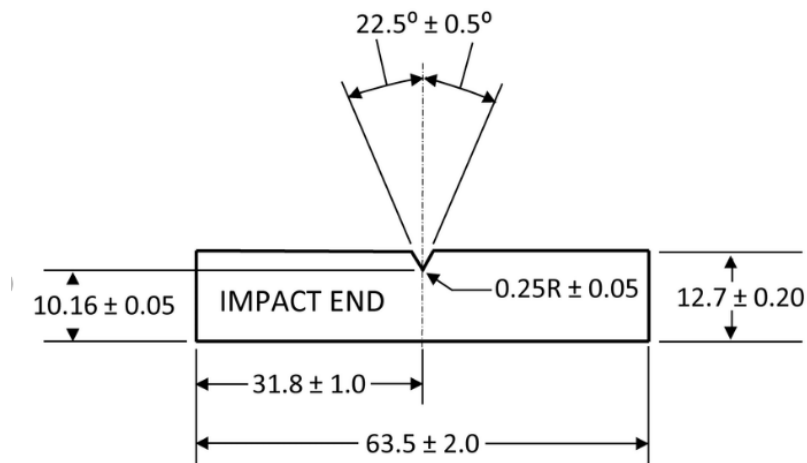


Figure 23. Dimensions of Izod impact test specimen.⁵⁶ All dimensions shown in millimeters.

3.3.4 Characterization by Scanning Electron Microscopy

Scanning electron microscopy was performed by a Phenom Pro (Thermo Fisher Scientific Inc., Waltham, Massachusetts, USA) scanning electron microscope. All samples were sputter coated with a gold/palladium mixture prior to imaging. Images were recorded from filament sides and ends. Filament samples were cryofractured prior to imaging. Filament samples were scored with a razor blade and then flash frozen in nitrogen for 10 minutes prior to fracturing. Blends containing TPU were etched with dimethylformamide by soaking TPU-containing blends in DMF for 24 hours. TPU blends were then removed from DMF and dried for an additional eight hours to allow DMF to fully evaporate. TPU etching was performed in order to dissolve the TPU component and allow for better visualization of the dispersion of TPU in the PLA matrix. SEM micrographs were recorded at approximately 300- and 6000-times magnification.

CHAPTER IV

4. RESULTS AND DISCUSSION I

PLA PROCESSING INVESTIGATION AND SINGLE-SCREW EXTRUSION OF PLA/TPU BLENDS

4.1 PLA Processing Investigations

In order to compare PLA/TPU blended filaments, we must first eliminate the effects of processing on material properties introduced by successive rounds of processing including extrusion, pelletizing, and injection molding. This section reports the investigation of the effects of various processing methods and post-processing steps on PLA properties. The different processing methods utilized were single-screw extrusion, twin-screw extrusion, and injection molding. Optimal processing parameters were obtained from the PLA material data sheet.¹¹ After processing, the different PLA variants underwent characterization. The characterization methods utilized were filament diameter measurement, TGA, DSC, tensile testing, and melt flow index rheology. Thermal analysis was performed on the PLA variants to investigate the effects of processing on material degradation and percent crystallinity. To ensure quality data was obtained during subsequent analysis, all pellets, filaments, and test bars were visually examined for defects and the diameter of filaments was measured to determine that filaments were within specifications.

4.1.1 PLA Pellet Appearance

Figure 24 shows PLA pellets that underwent different types of processing. Virgin PLA, single-screw PLA, and twin-screw PLA are compared below to see if extrusion processing and pelletizing had an effect on the pellet appearance. Visually there are minimal differences between the three variants, with the only difference being a minor variation in pellet size. This was attributed to a slight variation in speeds when the material was pelletized.



Figure 24. Appearance of virgin, single-screw, and twin-screw PLA pellets.

4.1.2 PLA Filament Appearance

Figure 25 shows the extruded filament. The diameters of the filament were measured to see if different processing methods had an effect on the diameter of the filaments. In Figure 28, PLA single-screw filament and PLA twin-screw filament appeared similar in opacity.

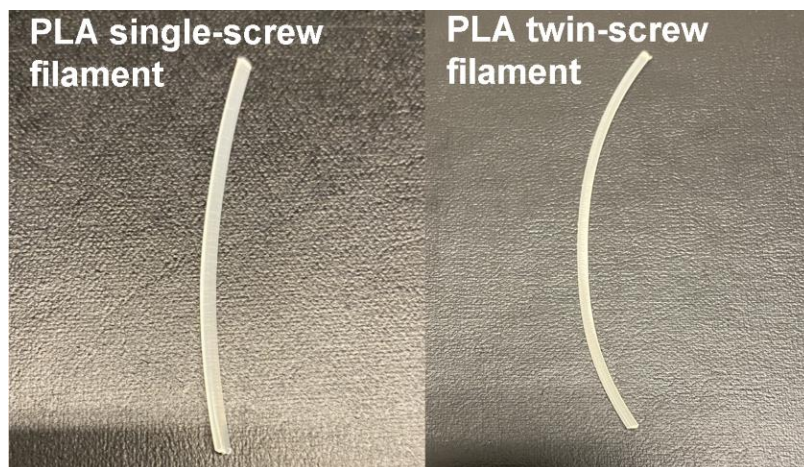


Figure 25. Appearance of single-screw and twin-screw PLA filament.

4.1.3 Filament Diameter Measurements

Filament was extruded on the single-screw and twin-screw extruder with the intent of achieving a desired 3D printing specification of 1.75 mm (± 0.05) in the 0° and 90° direction. Filament was measured with digital calipers in the 0° direction and the 90° degree direction approximately every two meters. An average diameter with standard deviation was reported. Measurement results for the PLA filament study are shown in table 5. According to table 5, single-screw PLA filament was not within the desired specifications of 1.75 mm (± 0.05) in the 0° and 90° direction. Twin-screw PLA filament was within specifications and was closer to a cylindrical profile than single-screw PLA filament. This is due to a greater stability of melt pressure during twin-screw extrusion versus single-screw extrusion.⁵⁷

Table 5. Filament Diameter Measurements of PLA Filaments

Sample	Diameter at 0° (mm)	Diameter at 90° (mm)
Single-screw PLA filament	1.67 (± 0.09)	1.63 (± 0.12)
Twin-screw PLA filament	1.76 (± 0.04)	1.72 (± 0.03)

Melt pressure is dictated by factors including rotational speed, screw dimensions, melt viscosity, and material interactions with the die.⁵⁸

4.1.4 PLA Sample Appearance

Figure 26 shows the injection-molded PLA samples produced by varying processing methods. There were few visual differences between the different processing methods. All injection-molded samples were opaque. It was determined that a difference in processing methods did not affect material appearance when PLA is utilized.

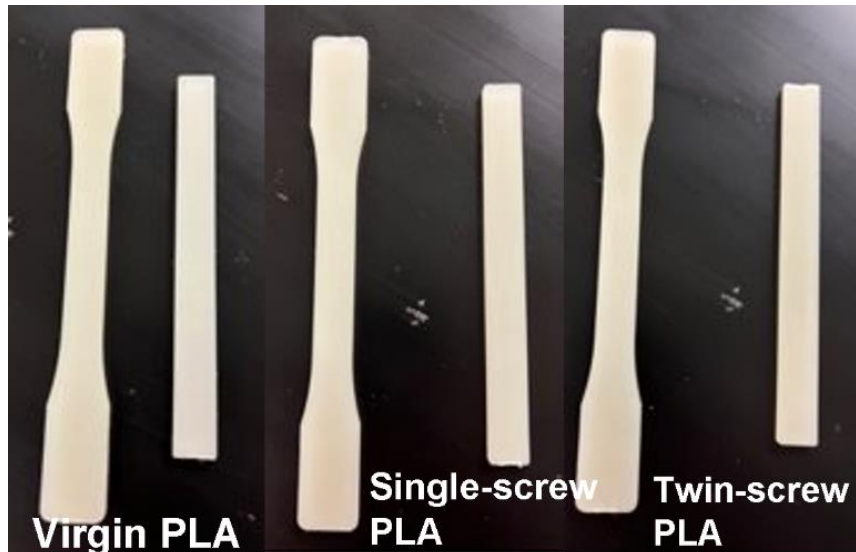


Figure 26. Appearance of virgin, single-screw, and twin-screw PLA injection-molded samples.

4.1.5 Thermogravimetric Analysis of PLA

The thermal stability of the PLA variants was investigated by TGA in a nitrogen atmosphere. Figure 27 displays the TGA thermograms of the PLA variants. The thermal properties of the PLA variants are summarized in Table 6.

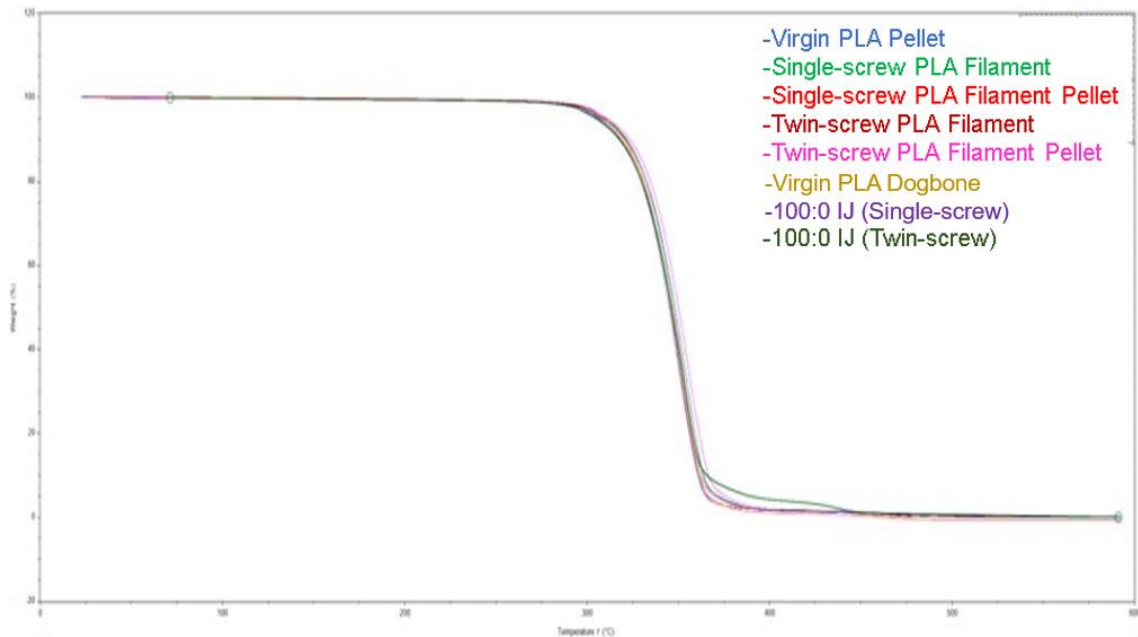


Figure 27. TGA thermograms of PLA through different processes. Virgin PLA pellet (—), Single-screw PLA filament (—), Single-screw PLA filament pellet (—), Twin-screw PLA filament (—), Twin-screw PLA filament pellet (—), Virgin PLA test bar (—), 100:0 IJ (Single-screw) (—), and 100:0 IJ (Twin-screw) (—).

Table 6. TGA Data of PLA Produced by Varied Processes

Formulation (%PLA/%TPU)	Temperature @ 10% Weight Loss (°C)	Temperature @ 50% Weight Loss (°C)	Percent Residue (%)
Virgin PLA Pellet	317	344	0.0
Single-Screw PLA Filament	318	344	0.0
Single-Screw PLA Filament Pellet	318	344	0.0
Twin-Screw PLA Filament	322	348	0.0
Twin-Screw PLA Filament Pellet	322	348	0.0
Virgin PLA Test Bar	319	346	0.0
Injection-molded PLA (from single-screw pellets)	321	348	0.0
Injection-molded PLA (from twin-screw pellets)	317	346	0.0

As demonstrated in table 6, there is no significant temperature difference between PLA variants at 10% weight loss or 50% weight loss. Similarly, there is no difference of percent residue among the different methods. The lack of difference shows that processing methods have minimal effects on PLA thermal stability.

4.1.6 Differential Scanning Calorimetry of PLA

The thermal behavior of PLA variants was investigated by DSC. Table 7 details the glass transition temperatures (T_g), crystallization temperatures (T_c), and melting temperatures (T_m) of PLA produced through varied processes.

Table 7. DSC Data of PLA Produced by Varied Processes

Formulation (%PLA/%TPU)	T_g (°C)	T_c (°C)	T_{m1} (°C)	T_{m2} (°C)	T_{m3} (°C)
Virgin PLA Pellet	65	103	144	159	176
Single-screw PLA Filament	64	114	144	171	177
Single-screw PLA Filament Pellet	65	109	144	169	176
Twin-screw PLA Filament	63	118	144	172	177
Twin-screw PLA Filament Pellet	64	119	144	173	177
Virgin PLA Test Bar	63	114	144	171	177
Injection-molded PLA (from single-screw pellets)	62	114	144	171	177
Injection-molded PLA (from twin-screw pellets)	62	113	143	170	176

Virgin PLA pellet shows significantly lower T_c and T_{m1} values compared to all other PLA variants studied. The remainder of the PLA variants show similar thermal transition values. The minimal differences among processed PLA variants show that the processing method had a minimal effect on PLA thermal transitions.

Crystallinity was calculated for each PLA variant according to Equation 1 shown below,⁵⁹ where $\Delta H_{m \text{ or } c}$ is enthalpy of melting or re-crystallization and ΔH_{m° is enthalpy of fusion of PLA (93.6 cal/g). Either the crystallization or melting peak was selected and the selected peak integrated using the TRIOS software to determine total enthalpy of melting or re-crystallization.

$$\frac{\Delta H_{m \text{ or } c}}{\Delta H_{m^\circ}} \times 100 = \% \text{ Crystallinity} \quad (1)$$

Table 8 below details the percent crystallinity calculated from T_m and T_c for each PLA variant.

Table 8. Percent Crystallinity of PLA from Varied Processes

Formulation (%PLA/%TPU)	Crystallinity Calculated from Melting (%)	Crystallinity Calculated from Recrystallization (%)
Virgin PLA Pellet	53.1	46.1
Single-screw PLA Filament	48.3	44.4
Single-screw PLA Filament Pellet	45.1	40.5
Twin-screw PLA Filament	57.0	51.2
Twin-screw PLA Filament Pellet	48.5	44.6
Virgin PLA Test Bar	54.4	46.1
Injection-molded PLA (from single-screw pellets)	45.8	44.6
Injection-molded PLA (from twin-screw pellets)	51.8	44.9

Crystallinity values for the PLA variants differ slightly among generations.

Single-screw PLA filament pellet had the lowest percent crystallinity from melting at 45.1%, while twin-screw PLA filament had the highest percent crystallinity from melting at 57%. All other PLA variants had crystallinity from melting between these values.

When crystallinity from recrystallization was examined, the overall difference between the highest percent crystallinity (twin-screw PLA filament: 51.2%) and the lowest percent crystallinity (single-screw PLA filament pellet: 40.5%) was similar to that of crystallinity from melting both in magnitude and trend.

4.1.7 Tensile Testing of PLA

Tensile testing was performed on the PLA variants to characterize mechanical properties. Table 9 displays the average tensile values of PLA variants. The values are an average of ten specimens per samples with standard deviation.

Table 9. Tensile Values of PLA Processed by Varied Methods

Formulation (%PLA/%TPU)	Modulus (Mpa)	Ultimate Elongation (%)
Single-screw PLA Filament	5347 (\pm 569)	2 (\pm 0.3)
Twin-screw PLA Filament	4911 (\pm 340)	2 (\pm 0.3)
Virgin PLA Test Bar	2243 (\pm 204)	3 (\pm 0.3)
Injection-molded PLA (from single-screw pellets)	2255(\pm 41)	3 (\pm 0.1)
Injection-molded PLA (from twin-screw pellets)	2286(\pm 49)	3 (\pm 0.1)

There are differences in the moduli between tensile filament and tensile bars. Tensile filament shared similar moduli values and tensile bars shared similar moduli values. The difference between filament and bars is attributed to a difference in sample geometry when testing.⁶⁰ There is negligible difference in the ultimate elongation of the PLA variants. This table shows that a differences in processing methods has minimal effects on the tensile properties of PLA variants with a specific sample geometry (filament versus test bar).

4.1.8 Melt Flow Index Rheology of PLA

Melt flow index rheology was performed on PLA variants to observe if utilizing different processing methods had an effect of the melt flow of PLA. Table 10 shows the melt flow index values of the PLA variants.

Table 10. Melt Flow Index of PLA through Different Processes

Formulation (%PLA/%TPU)	Melt Flow Index (g/10 min)
Literature Value of PLA	9-15
Virgin PLA pellet	16.1 (± 1.1)
Single-screw PLA Filament pellet	14.8 (± 1.2)
Twin-screw PLA Filament pellet	13.4 (± 0.7)

Minimal differences were present among the MFI values of virgin PLA pellet, single-screw PLA filament pellet, and twin-screw PLA filament pellet. The differences can be attributed to minor mechanical chain scission during the extrusion and regrinding process, if molecular weight changes are present at all.⁶¹ Despite the small differences, MFI values are similar to the range reported in the literature. For all practical purposes, processing method has minimal effects on melt rheology for PLA variants.

4.2 Single-screw Extrusion Processing of PLA/TPU Blends

The different blend ratios were evaluated in comparison to their virgin counterparts. The YellowJacket industrial scale single-screw extruder was used to process all materials evaluated in this section. All filament blends were extruded at optimal parameters^{11,18}. These parameters were determined by the values specified on the material data sheets.^{11,18} All materials were extruded into filament on the YellowJacket and were subject to further testing and analysis.

All single-screw extruded filament was examined for defects and their diameters were measured to investigate if the filaments were within specification. The extruded filament underwent characterization by diameter measurement, TGA, DSC, tensile testing, and SEM. Thermal analysis was performed on the virgin pellet and extruded filament by TGA and DSC to investigate the effects of processing on thermal properties of the blends. SEM analysis was performed on filament blends to investigate the distribution of TPU within the PLA matrix.

4.2.1 Extruded Filament Appearance

Figure 28 shows the appearance of extruded filament. Filament blends were separated into two categories for subsequent analysis. One subsection focused on the geometry optimization of the filament blends while the other focused on the material behavior transition from rigidity to elasticity. In Figure 32, 100/0 filament blend appeared to be opaque, along with 90/10, 70/30, 50/50, 30/70 and 10/90 filament blends. The 0/100 filament blends appeared to be translucent. The opaqueness of the filament blends is due to PLA within the filament blends being semi-crystalline in nature⁶². Semi-crystalline polymers generally do not allow light to be transmitted and is instead reflected by the

crystallites that are larger than the wavelength of light present within the system, causing an opaque appearance⁶². 0/100 appears translucent in nature due to the absence of crystallites within its matrix⁶².

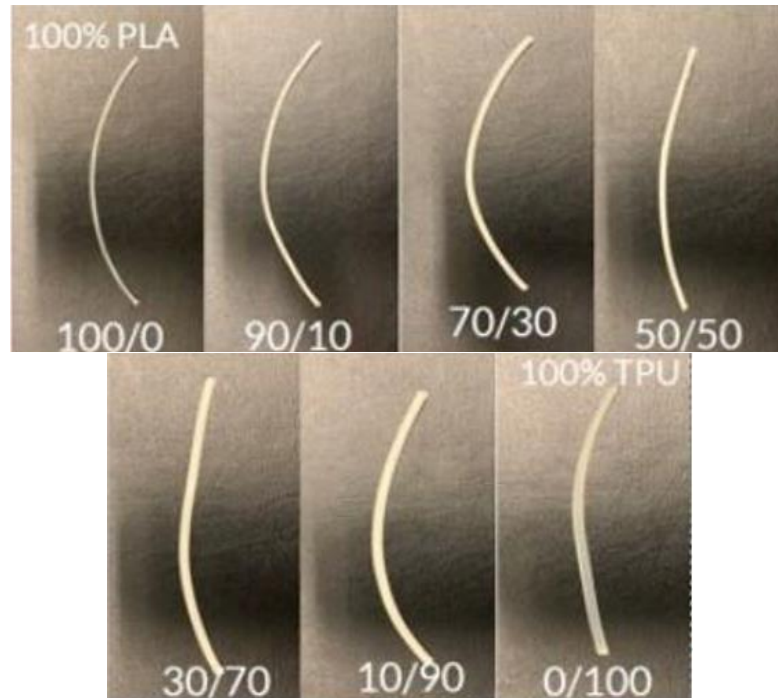


Figure 28. Appearance of individual PLA/TPU filaments – optimization.

In Figure 29, 70/30, 65/35, 60/40, 55/45/, 50/50, 45/55, 40/60, 35/65, and 30/70 filament blends appeared to be opaque in nature. The opaqueness of the filament blends is due to presence of PLA crystalline domains within the filament, similar to the blends shown in Figure 28 above.

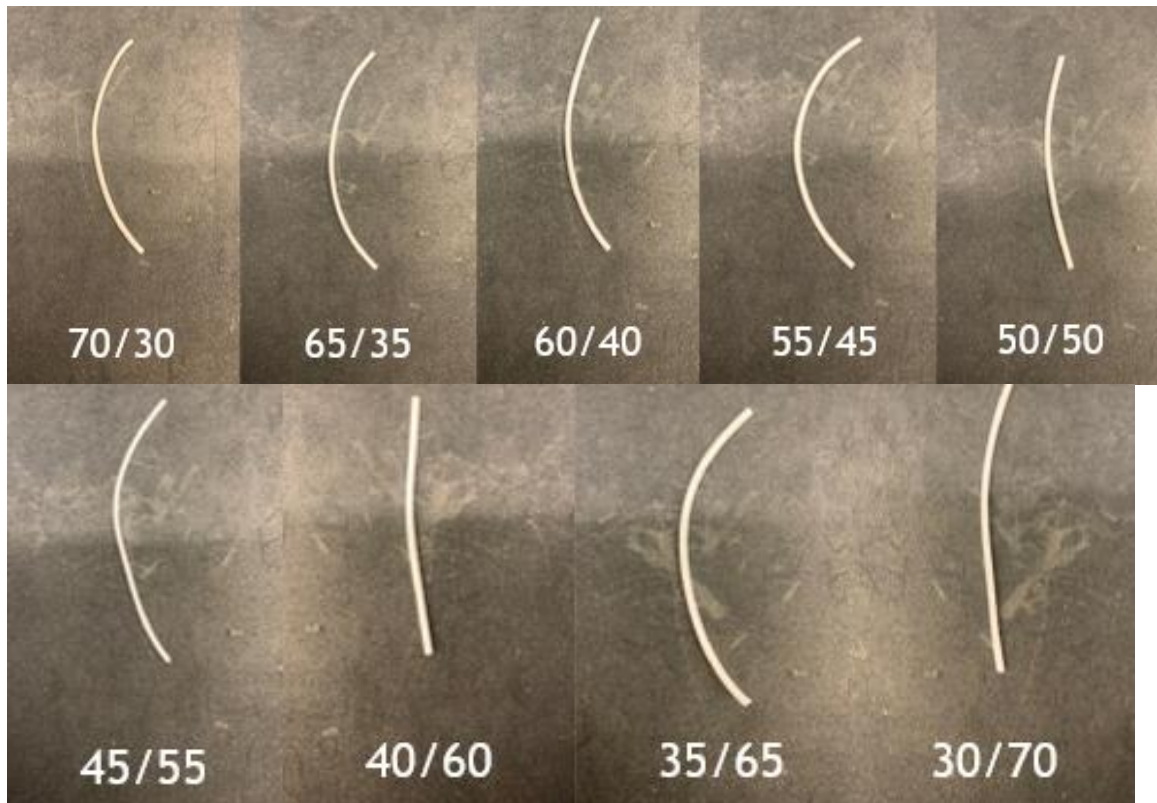


Figure 29. Appearance of individual PLA/TPU Filaments focusing on the plastic-to-elastic material transition.

4.2.2 Filament Diameter Measurements

Filament was extruded on the single-screw extruder with the intent of reaching a desired specification of 1.75 mm (± 0.05) in the 0° and 90° direction. Measurement results for the optimization section are shown in table 11. According to table 11, none of the “optimized” filament blends from single-screw extrusion were within the desired specifications of 1.75 mm (± 0.05) in the 0° and 90° direction. Additionally, blends with higher PLA concentrations were far from cylindrical. This is due to varying melt pressure values while using the YellowJacket single-screw extruder and a lack of elastic memory from PLA⁶³. Blends containing higher concentrations of TPU also did not meet specifications but were closer to being cylindrical. This is due to TPU having elastic

memory, allowing the filament extrusion process to not be affected as much by variations in melt pressure.⁶³

Table 11. Filament Diameter Measurements of Optimization Filaments

Formulation (%PLA/%TPU)	Diameter at 0° (mm)	Diameter at 90° (mm)
100/0	1.78 (±0.08)	1.90 (±0.05)
90/10	1.74 (±0.18)	1.76 (±0.17)
70/30	1.79 (±0.08)	1.80 (±0.08)
50/50	1.71 (±0.08)	1.77 (±0.07)
30/70	1.91 (±0.03)	1.87 (±0.04)
10/90	1.58 (±0.05)	1.61 (±0.05)
0/100	1.67 (±0.16)	1.68 (±0.18)

Measurement results for blends extruded while studying the plastic-to-elastic transition are shown in table 12. According to table 12, none of the filament blends from the plastic to elastic section reached the desired specifications of 1.75 mm (±0.05) in the 0° and 90° directions. In addition to not reaching the desired specifications, blends containing higher concentrations of PLA were not cylindrical for similar reasons as the optimized filament blends. Similarly, blends containing higher concentrations of TPU also did not meet specifications but were more cylindrical.

Table 12. Filament Diameter Measurements of Plastic-to-elastic Filaments

Formulation (%PLA/%TPU)	Diameter at 0° (mm)	Diameter at 90° (mm)
70/30	1.79 (±0.08)	1.80 (±0.08)
65/35	1.66 (±0.05)	1.68 (±0.04)
60/40	1.78 (±0.06)	1.78 (±0.05)
55/45	1.80 (±0.05)	1.77 (±0.03)
50/50	1.71 (±0.08)	1.77 (±0.03)
45/55	1.94 (±0.09)	1.91 (±0.05)
40/60	1.78 (±0.10)	1.68 (±0.10)
35/65	1.69 (±0.09)	1.63 (±0.11)
30/70	1.91 (±0.03)	1.87 (±0.04)

4.2.3 Thermogravimetric Analysis of PLA/TPU blends

The thermal stability of all PLA/TPU blends was investigated by TGA in a nitrogen atmosphere. Figure 30 displays the TGA thermograms of the optimized single-screw filament blends. The thermal properties of the PLA/TPU optimization blends are summarized in Table 13.

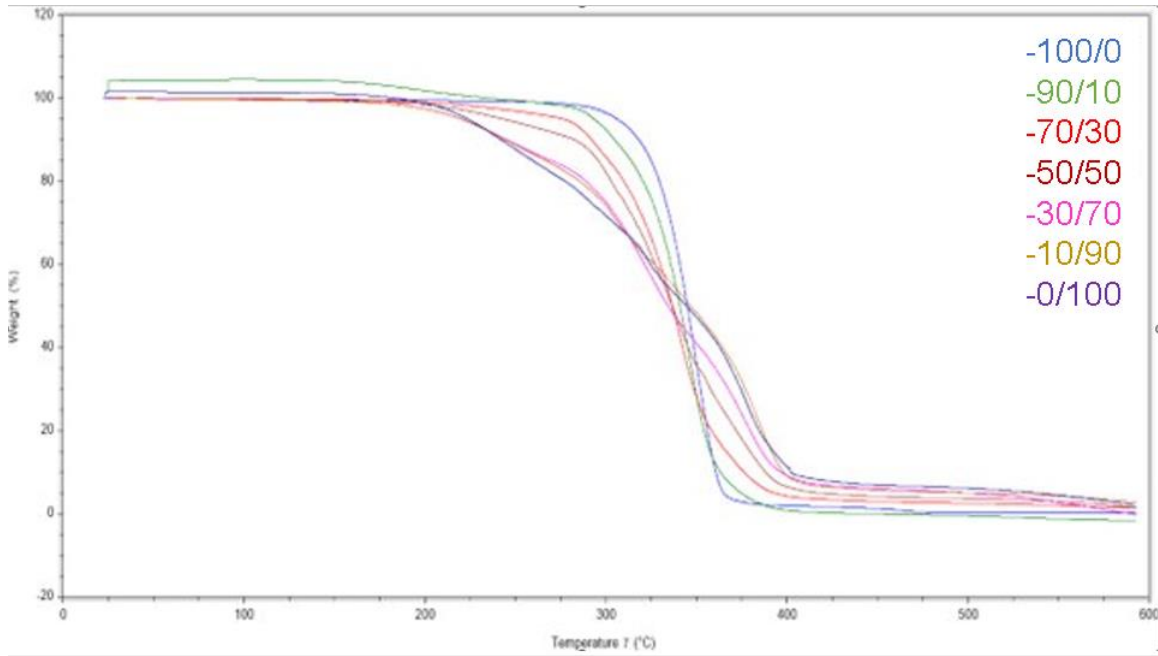


Figure 30. TGA thermograms of the PLA/TPU single-screw optimization blends. 100/0 (—), 90/10 (—), 70/30 (—), 50/50 (—), 30/70 (—), 10/90 (—), and 0/100 (—).

Table 13. Thermal Properties of PLA/TPU Optimization Blends

Formulation (%PLA/%TPU)	Temperature @ 10% Weight Loss (°C)	Temperature @ 50% Weight Loss (°C)	Percent Residue (%)
100/0	318	345	0.2
90/10	305	341	0
70/30	292	337	1.3
50/50	250	328	0
30/70	245	334	0
10/90	245	347	2.1
0/100	242	345	2.1

As TPU content increases within a blend, a clear decrease in thermal stability was shown at 10% weight loss. The trend was similar at 50% weight loss. As TPU content

increases, the rate of decomposition decreased, as demonstrated by the larger differences between 10% weight loss and 50% weight loss as TPU content increased. There was a slight increase in percent residue at the highest TPU incorporation levels.

Figure 31 displays the TGA thermograms of the single-screw plastic-to-elastic section. The thermal properties of the PLA/TPU optimization blends are summarized in Table 14.

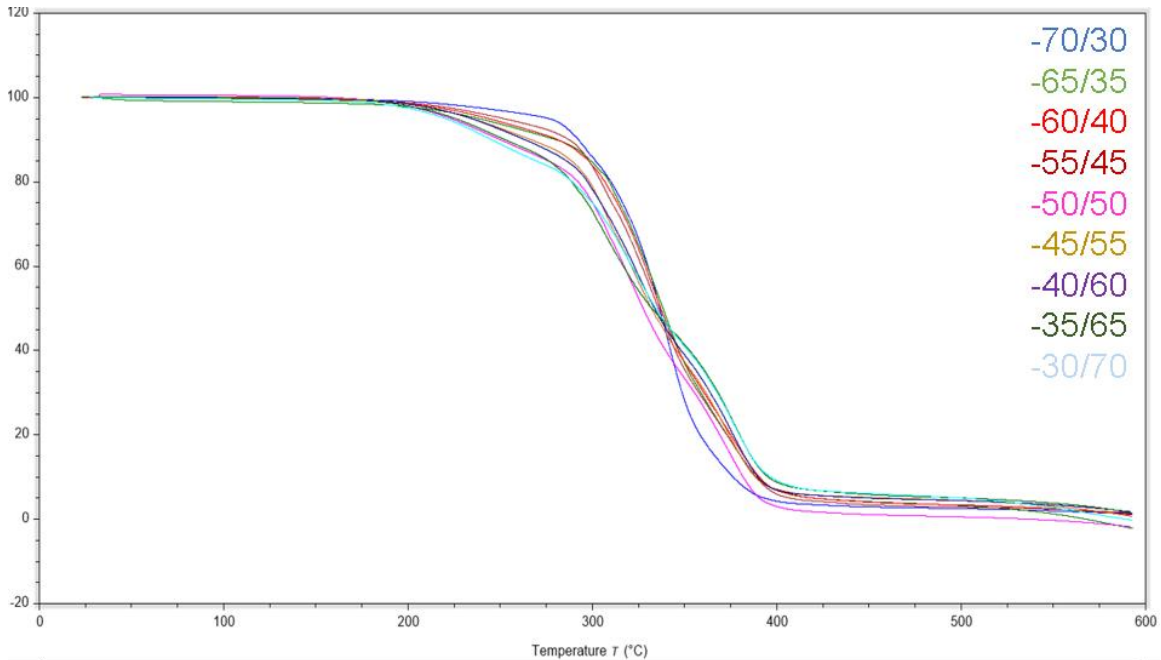


Figure 31. TGA thermograms of the PLA/TPU single-screw plastic-to-elastic blends. 70/30 (—), 65/35 (—), 60/40 (—), 55/45 (—), 50/50 (—), 45/55 (—), 40/60 (—), 35/65 (—), and 30/70 (—).

Table 14. Thermal Properties of PLA/TPU Plastic-to-elastic Blends

Formulation (%PLA/%TPU)	Temperature @ 10% Weight Loss (°C)	Temperature @ 50% Weight Loss (°C)	Percent Residue (%)
70/30	292	337	1.3
65/35	280	338	0.0
60/40	281	337	1.1
55/45	287	335	1.5
50/50	250	328	0.6
45/55	267	332	4.5
40/60	263	334	4.4
35/65	253	332	5.0
30/70	245	334	5.0

Similar to the optimization blends, as TPU content increased within a blend, a clear decrease in thermal stability was apparent at 10% weight loss. The trend is similar at 50% weight loss. The rate of decomposition decreased as TPU increased, similar to optimized filament blends.

4.2.4 Differential Scanning Calorimetry of PLA/TPU Blends

The thermal behavior of PLA/TPU blends was investigated by DSC. Figure 32 shows a DSC curve of the 70/30 blend as an example of the typical features we observed in our DSC curves.

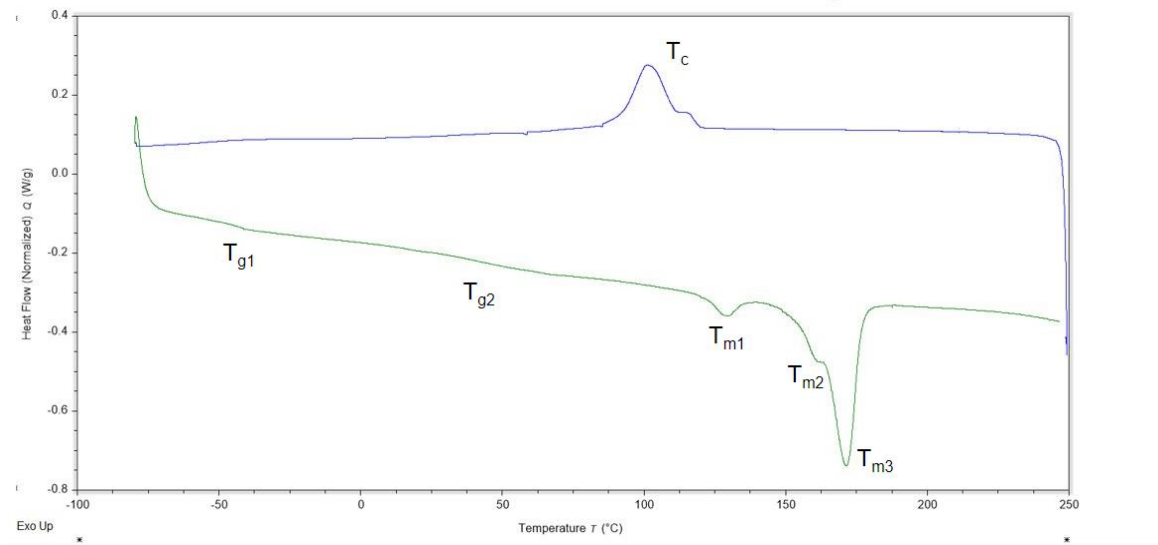


Figure 32. The cool down and second heat curves for 70/30 filament.

Table 15 displays the thermal transitions for PLA/TPU optimization blends. As concentrations of TPU increased within a filament, a clear decrease in T_g was observed. T_c also shows a clear decrease in value as TPU content increased. T_m also followed a similar trend.

Table 15. DSC Values of Optimization Blends

Formulation (%PLA/%TPU)	T _{g1} (°C)	T _{g2} (°C)	T _c (°C)	T _{m1} (°C)	T _{m2} (°C)	T _{m3} (°C)
100/0	63.45	-----	113.46	144.43	169.95	176.25
90/10	-43.46	47.94	109.44	-----	166.52	175.01
70/30	-41.51	48.92	104.50	-----	163.41	172.68
50/50	-45.60	63.48	95.53	-----	157.75	168.96
30/70	-45.41	63.65	85.37	-----	-----	164.06
10/90	-45.90	-----	82.60	141.27	160.06	-----
0/100	-46.67	-----	83.26	-----	-----	148.23

Table 16 displays the plastic to elastic values for PLA/TPU blends investigated by DSC. The T_g, T_c, and T_m followed a similar trend to the optimized filament blends.

Table 16. DSC Values of Plastic-to-elastic Blends

Formulation (%PLA/%TPU)	T _{g1} (°C)	T _{g2} (°C)	T _c (°C)	T _{m1} (°C)	T _{m2} (°C)
70/30	-41.51	47.07	104.50	163.41	172.68
65/35	-45.48	64.15	98.85	160.35	171.34
60/40	-44.99	65.76	96.25	158.73	169.89
55/45	-44.70	65.72	96.13	158.71	170.11
50/50	-44.66	63.48	94.81	157.05	168.86
45/55	-45.45	61.97	87.03	-----	166.58
40/60	-43.11	64.73	86.40	147.26	166.78
35/65	-45.48	64.21	83.72	-----	164.23
30/70	-45.41	63.65	85.37	-----	164.06

In table 17, there are two sections, overall crystallinity and PLA fraction crystallinity. Overall crystallinity is calculated by the equation shown in figure 31. To determine whether this was due to a dilution effect when TPU was incorporated or if TPU had additional effects on crystallinity, the overall crystallinity values were divided by the weight percent of PLA within the system.

Table 17: Percent Crystallinity of Optimization Blends

Formulation (%PLA/%TPU)	Overall Crystallinity from Melting (%)	PLA Fraction Crystallinity Fraction from Melting (%)	Overall Crystallinity from Recrystallization (%)	PLA Fraction Crystallinity Fraction from Recrystallization (%)
100/0	49.5	49.5	44.5	44.5
90/10	44.8	49.7	40.7	45.2
70/30	36.5	52.1	32.3	46.1
50/50	29.1	58.2	28.7	57.4
30/70	14.4	48.0	16.3	54.3
10/90	5.7	57.0	4.8	48.0

Table 17 shows a steady decrease in overall crystallinity from melting and recrystallization as increasing amounts of TPU are incorporated into the filament blends. PLA fraction crystallinity increases as TPU is incorporated into the blends, until 30/70 where it decreases. Crystallinity continues to increase after this in blend 10/90.

Table 18: Percent Crystallinity of Plastic-to-elastic Blends

Formulation (%PLA/%TPU)	Overall Crystallinity from Melting (%)	PLA Fraction Crystallinity Fraction from Melting (%)	Overall Crystallinity from Recrystallization (%)	PLA Fraction Crystallinity Fraction from Recrystallization (%)
70/30	36.5	52.1	32.3	46.1
65/35	42.7	65.6	40.5	62.3
60/40	30.4	50.6	29.1	48.5
55/45	30.1	54.7	26.2	47.6
50/50	29.1	58.2	28.7	57.4
45/55	19.6	43.4	18.4	40.8
40/60	28.4	71.0	25.0	62.5
35/65	16.4	46.8	14.7	42.0
30/70	14.4	48.0	16.3	54.3

Table 18 shows a steady decrease in overall crystallinity from melting and recrystallization as increasing amounts of TPU are incorporated into the filament blends. PLA fraction crystallinity sharply increases in blend 65/35. There is a sharp decrease in PLA fraction crystallinity at blend 60/40. PLA fraction crystallinity increases with the incorporation of TPU, until 35/60 where it decreases and shows minimal change in 30/70.

4.2.5 Tensile Testing of PLA/TPU Blends

Tensile testing was performed on PLA/TPU filament blends to characterize mechanical properties. Table 19 displays the average tensile values of optimized filament blends. The values are an average of ten specimens per samples with standard deviation.

Table 19. Tensile Values of PLA/TPU Optimization Blends

Formulation (%PLA/%TPU)	Modulus (MPa)	Ultimate Elongation (%)
100/0	5762 (± 1025)	5.4 (± 1.2)
90/10	4729 (± 579)	111 (± 62)
70/30	3627 (± 230)	150 (± 0)
50/50	2056 (± 169)	483 (± 32)
30/70	18.5 (± 2.2)	258 (± 24)
10/90	4.5 (± 1.0)	512 (± 13)
0/100	8.8 (± 1.5)	240 (± 27)

As TPU concentration increased within a blend, filament modulus decreased. Elongation followed an inverse trend with the increase in TPU; elongation increased as the concentration of TPU increased. This occurred because of the composition of the TPU within the system. As TPU concentrations increased, so did the amount of soft segments of TPU within the system which attributed to an increase of material flexibility and decrease in material rigidity.⁶⁴

Table 20 displays the average tensile values of plastic-to-elastic filament blends. The values are an average of ten specimens per samples with standard deviation.

Table 20. Tensile Values of PLA/TPU Plastic-to-elastic Blends

Formulation (%PLA/%TPU)	Modulus (Mpa)	Ultimate Elongation (%)
70/30	3627 (± 230)	145 (± 10)
65/35	2378 (± 210)	263 (± 68)
60/40	2240 (± 423)	296 (± 54)
55/45	3006 (± 403)	287(± 149)
50/50	2056 (± 169)	483 (± 32)
45/55	1643 (± 924)	437 (± 13)
40/60	1376 (± 365)	152 (± 36)
35/65	819 (± 579)	146 (± 47)
30/70	18.5 (± 2.2)	258 (± 24)

Plastic-to-elastic filament blends demonstrated similar trends in mechanical properties as optimized blends. There was a clear decrease of the moduli as more TPU

was incorporated within the blends. This trend was shared with ultimate strength. An inverse trend was shown with ultimate elongation.

4.2.6 SEM Characterization of PLA/TPU Blends

SEM was performed on PLA/TPU filament blends to observe the effective distribution of TPU within the PLA filament matrix. Each blend was soaked in DMF and cryofractured with liquid nitrogen to observe the TPU domains within the system. Figure 33 displays the SEM micrographs of optimized filaments. Table 21 shows the TPU domain size of the optimized filaments measured from the SEM micrographs.

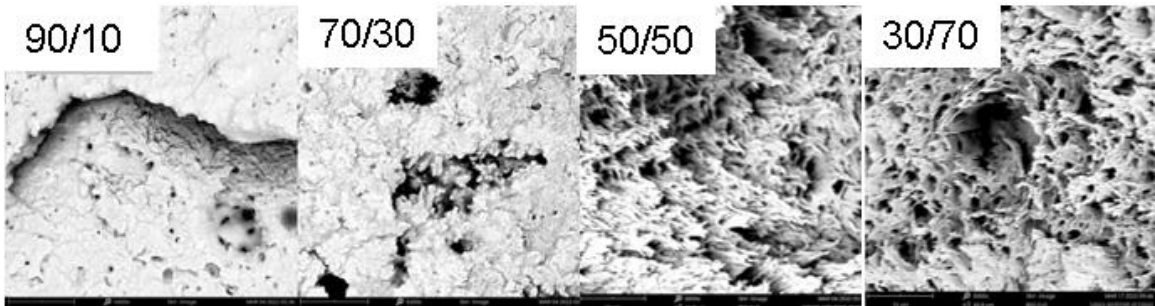


Figure 33. SEM micrographs of PLA/TPU Optimized blends at approximately 6000x magnification.

Table 21. Domain Size of TPU Domains in Optimized Filaments

Formulation (%PLA/%TPU)	Domain Size (nm)
90/10	1191 (± 274)
70/30	1306 (± 356)
50/50	1080 (± 324)
30/70	924 (± 233)

As the ratio of TPU within a blend increased, the size of the domains decreased while the number of TPU domains increased.

Figure 34 displays the SEM micrographs of the plastic to elastic section. Table 21 shows the TPU domain size of the optimized filaments measured from the SEM micrographs.

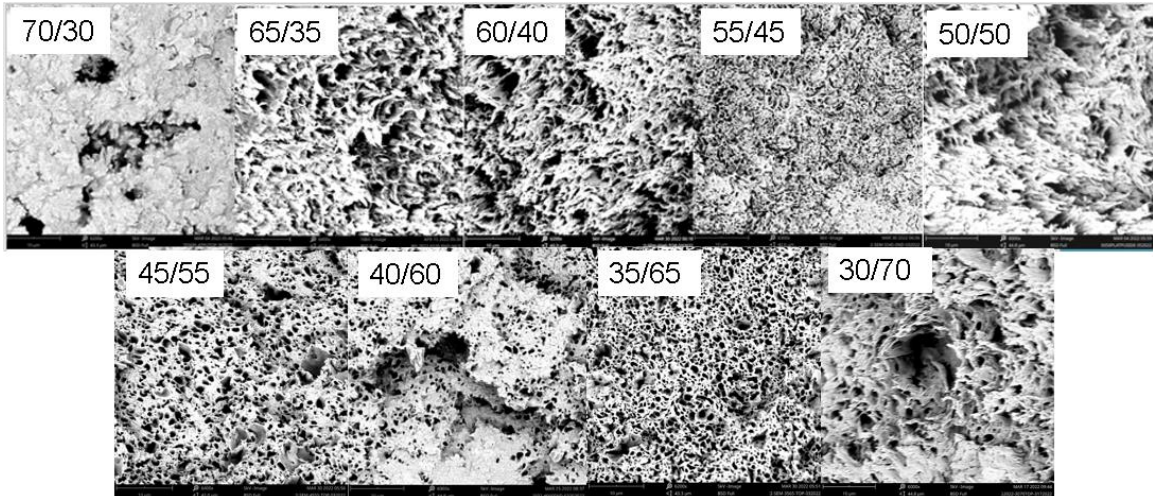


Figure 34. SEM micrographs of PLA/TPU plastic-to-elastic blends at approximately 6000x magnification.

Table 22. Domain Size of TPU Domains in Plastic-to-elastic Filaments

Formulation (%PLA/%TPU)	Domain Size (nm)
70/30	1306 (± 356)
65/35	1201 (± 324)
60/40	1269 (± 241)
55/45	1004 (± 170)
50/50	1080 (± 323)
45/55	901 (± 191)
40/60	817 (± 93)
35/65	767 (± 133)
30/70	924 (± 233)

Similar to optimized filaments, as the ratio of TPU within a blend increased, the size of the domains decreased while the number of TPU domains increased.

4.3 Summary

PLA variants were successfully processed using the Yellowjacket single-screw extruder and Arburg injection molder. Pellet and filament appearances of PLA showed that there are minimal differences between different processing methods. Thermal characterization by TGA showed that there are minimal differences between material variants. Thermal analysis by DSC showed that there are slight differences in T_c and T_{m2} values of virgin PLA pellet compared to the remainder of the PLA variants. Aside from

these two values, there were minimal differences between PLA variants. Percent crystallinity analysis of PLA showed that crystallinity varied over the different processing methods by 10 to 12% based on the type of crystallinity considered. Tensile testing of PLA showed similar moduli for filament variants and similar moduli for test bar variants and differences were attributed to sample geometry. Melt flow index rheology of PLA variants showed minimal differences between different pellet variants.

PLA/TPU blends were successfully processed using the Yellowjacket single-screw extruder. Visually, the majority of filament blends were opaque in appearance besides 0/100, which was translucent. Filament diameter measurement of optimization and plastic-elastic blends show that these blends did not meet the required specifications of 1.75 mm (± 0.05) in the 0° and 90° direction, but blend cylindricality did improve with the incorporation of TPU. Thermal analysis by TGA shows a steady decrease in thermal stability in both optimization and plastic-elastic blends with increased TPU. The rate of decomposition decreased as TPU was incorporated.

Thermal analysis of optimization filament blends by DSC showed a clear decrease in the glass transition temperatures with TPU incorporation. With this TPU incorporation, additional glass transition temperatures were identified. Optimization blends that showed two glass transition temperatures were 90/10, 70/30, 50/50, and 10/90. In blend 90/10, it shows two glass transition temperatures, with the first one similar in value to that of Virgin TPU. The second glass transition temperature, which was expected to be closer in value to Virgin PLA, was approximately 15 °C lower. This was also observed in 70/30 and suggests that partial miscibility was accomplished in these blends. The second glass transition temperatures returned to values closer to Virgin

PLA following these blends, showing that the blends returned to being completely immiscible. Crystallization temperatures in optimization blends were observed to decrease steadily with TPU incorporation. Melt temperatures showed a decrease with TPU incorporation. There were minimal differences in the second and third melt temperatures of optimization blends. It is important to note that a handful of optimization blends did not display all three melting transitions evident in Virgin PLA. DSC values of plastic-to-elastic values showed similar glass transition values with TPU incorporation. Each plastic-to-elastic blend exhibited a second glass transition temperature, with blend 70/30 being the only blend that suggests partial miscibility. Plastic-to-elastic crystallization temperatures decreased steadily with TPU incorporation. Plastic-to-elastic melt temperatures decreased steadily with TPU incorporation. Percent crystallinity analysis showed a clear decrease in overall crystallinity from melting and recrystallization in optimization and plastic-elastic blends. PLA fraction crystallinity increased with TPU incorporation, until 30/70 in optimization and 35/65 in plastic-elastic. Tensile testing of optimization and plastic-elastic blends showed a steady decrease in material modulus with increased TPU content, with a sharp decrease in modulus at 30/70 PLA/TPU. SEM characterization of optimization and plastic-elastic blends showed decreased TPU domain size and increased number of TPU domains as TPU incorporation increased.

CHAPTER V

5. RESULTS AND DISCUSSION II

TWIN-SCREW EXTRUSION AND INJECTION MOLDING OF PLA/TPU BLENDS

5.1 Twin-screw Extrusion Processing

The different blend ratios were evaluated in comparison to their single-screw counterparts. The LabTech industrial scale twin-screw extruder was used to process all materials evaluated in this work. All filament blends were extruded at optimal parameters.¹¹ To ensure quality data was obtained during subsequent analysis, all extruded filament was examined for defects and their diameters were measured to investigate if the filaments were within specification. All materials were extruded into filament and were subject to further testing and analysis. The extruded filament underwent characterization by diameter measurement, TGA, DSC, tensile testing, and SEM. Thermal analysis was performed on the extruded filament by TGA to investigate the effects of processing on material degradation. DSC analysis was performed to determine the effect of processing on thermal transitions among the blends. SEM imaging was performed on filament blends to investigate the distribution of TPU within the PLA matrix.

5.2 Appearance of PLA/TPU Pellets

Figure 35 shows the differing pellet blends. 100/0, 90/10, 70/30, 50/50, 30/70, 10/90, and 0/100 were compared below to see if processing by twin-screw extrusion had an effect on the appearance of the pellets. Visually, there was minimal differences between the blends. The only difference was a variation in pellet size in 10/90 and 0/100 pellet blends due to an increasing amount of elasticity which caused the regrind machine to stretch and tear the strands rather than cut them.



Figure 35. Appearance of 100/0, 90/10, 70/30, 50/50, 30/70, 10/90, and 0/100 twin-screw pellets.

5.3 Appearance of PLA/TPU Filaments

Figures 36 shows the extruded twin-screw filament. The diameters of the filament were measured to see if twin-screw extrusion had an effect in the diameter of the filaments. In Figure 36, 100/0, 90/10, 70/30, 50/50, 30/70, and 10/90 blends appear to be visually opaque. 0/100 blend appears to be translucent.

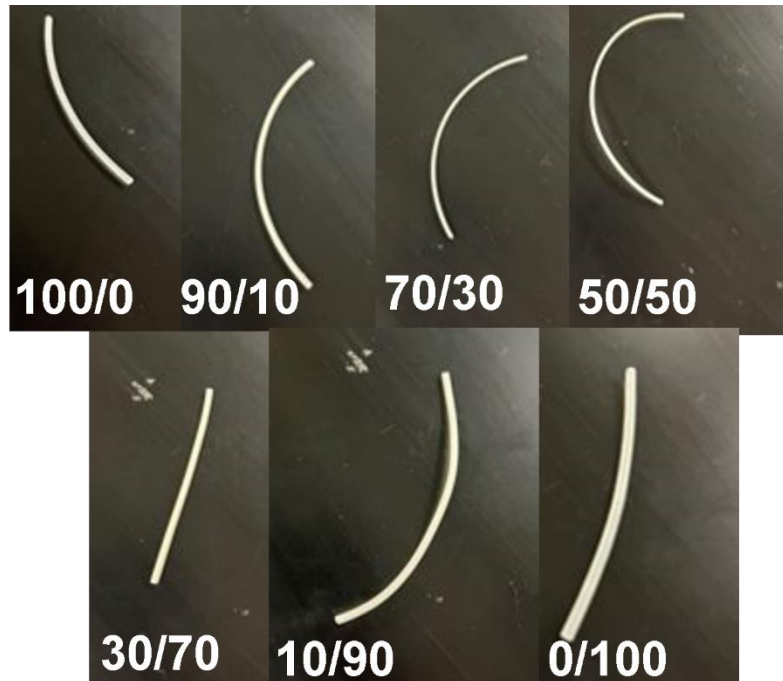


Figure 36. Appearance of 100/0, 90/10, 70/30, 50/50, 30/70, 10/90, and 0/100 twin-screw pellets.

5.4 Filament Diameter Measurements

Filament was extruded on the twin-screw extruder with the intent of reaching a desired specification of 1.75 mm (± 0.05) in the 0° and 90° direction. This specification requirement was set with the intent of utilizing the filament for 3D printing. Filament measurements were performed similarly to single-screw extruded filaments.

Measurements for the twin-screw filament blends are shown in table 23.

Table 23. Twin-screw Filament Diameter Measurements

Formulation (%PLA/%TPU)	0 degrees (mm)	90 degrees (mm)
100/0	1.76 (± 0.04)	1.72 (± 0.03)
90/10	1.88 (± 0.02)	1.88 (± 0.03)
70/30	1.64 (± 0.03)	1.64 (± 0.04)
50/50	1.88 (± 0.02)	1.88 (± 0.03)
30/70	1.70 (± 0.03)	1.72 (± 0.03)
10/90	1.88 (± 0.02)	1.87 (± 0.03)
0/100	1.76 (± 0.06)	1.74 (± 0.05)

Two of the filament blends were within the desired specifications of 1.75 mm (± 0.05) in the 0° and 90° direction. These blends were 100/0 and 0/100. Compared to

single-screw extrusion, all blends had a profile that was more consistently cylindrical due to consistent melt pressure. Even though most blends were out of specifications, they can easily reach specifications with the modification of process parameters. On the twin-screw extruder, screw speed can be varied to improve geometry. On the puller/winder takeoff speed and traction percentage can be varied.

5.5 Thermogravimetric Analysis of Twin-screw Blends

The thermal stability of the PLA/TPU blends extruded by twin-screw extrusion was investigated by TGA. Figure 37 displays the TGA thermograms of the twin-screw blends. The thermal properties of the PLA/TPU blends are summarized in Table 24.

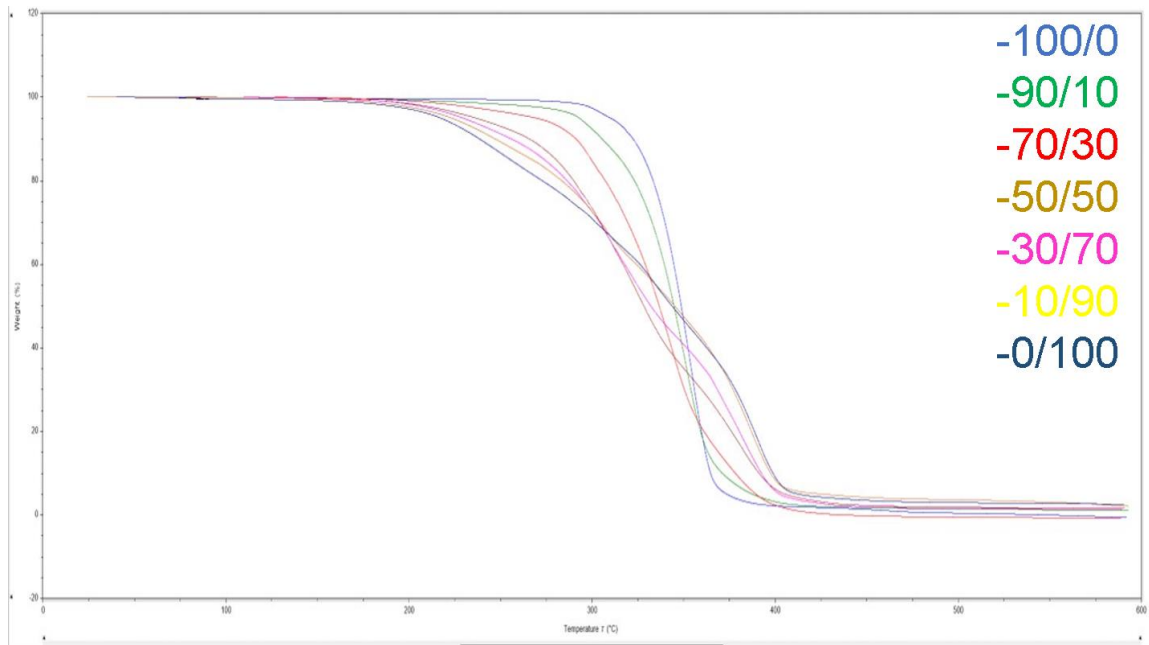


Figure 37. TGA thermograms of twin-screw PLA/TPU filament blends: 100/0 (—), 90/10 (—), 70/30 (—), 50/50 (—), 30/70 (—), 10/90 (—), and 0/100 (—).

Table 24. Thermal Properties as Determined by TGA of Twin-screw Filament Blends

Formulation (%PLA/%TPU)	Temperature @ 10% Weight Loss (°C)	Temperature @ 50% Weight Loss (°C)	Percent Residue (%)
100/0	322	349	0.0
90/10	305	345	1.1
70/30	291	337	0.0
50/50	266	328	1.6
30/70	256	332	1.4
10/90	247	345	2.1
0/100	239	343	2.5

As TPU content increases within the blends, a clear decrease in thermal stability was shown at 10% weight loss. The trend is similar at 50% weight loss. As TPU content increases, the rate of decomposition decreased, as demonstrated by the larger differences between 10% weight loss and 50% weight loss as TPU content increased.

5.6 Differential Scanning Calorimetry of Twin-screw Filament Blends

The thermal behavior of twin-screw extruded PLA/TPU blends was investigated by DSC. Table 25 displays the twin-screw values for filaments blends.

Table 25. Thermal Properties as Determined by DSC for Twin-screw Filament Blends

Formulation (%PLA/%TPU)	T _{g1} (°C)	T _{g2} (°C)	T _c (°C)	T _{m1} (°C)	T _{m2} (°C)	T _{m3} (°C)
100/0	64	-----	109	143	170	176
90/10	58	-----	110	-----	168	175
70/30	-44	47	104	-----	163	172
50/50	-44	35	92	-----	167	-----
30/70	-46	-----	85	-----	165	-----
10/90	-45	-----	81	-----	160	-----
0/100	-45	-----	78	141	159	-----

As concentrations of TPU increased within a filament, a clear decrease in T_g was observed. As more TPU is incorporated within the blends, a second T_g appears on the DSC curve of 50/50 and 70/30. This second T_g shows in polymer systems which are immiscible. The presence of two glass transition temperature proves they do not mix at a molecular level and maintain a separate glass transition.⁶⁵ T_c also showed a clear decrease in value as TPU content increased. T_m also followed a similar trend. The decrease in

thermal stability can be attributed to a few factors. Greater concentrations of TPU within the system contributed to an overall decrease in thermal stability due to TPU being an amorphous polymer. Amorphous polymers have lower glass transition temperatures and lower melting temperatures compared to semi-crystalline polymers. Thermal stability in semi-crystalline polymers is attributed to crystallinity. Crystals require a greater amount of thermal energy to transition from solid polymer to the molten phase. Since crystallinity naturally decreases as the ratio of amorphous polymer increases, this explains the decrease in thermal transition temperatures.⁶⁶

Overall crystallinity was calculated for twin-screw extruded PLA/TPU blends using Equation 1 presented previously. The heat of melting and heat of re-crystallization was determined from DSC curves of these blends. Crystallinity of the PLA fraction was calculated by dividing the overall crystallinity value by the weight percentage of PLA in the blend.

Table 26: Percent Crystallinity of Twin-screw Filament Blends

Formulation (%PLA/%TPU)	Overall Crystallinity from Melting (%)	PLA Fraction Crystallinity Fraction from Melting (%)	Overall Crystallinity from Recrystallization (%)	PLA Fraction Crystallinity Fraction from Recrystallization (%)
100/0	52.2	52.2	48.4	48.4
90/10	42.0	46.6	40.1	44.5
70/30	32.7	46.7	31.3	44.7
50/50	24.8	49.6	22.8	45.6
30/70	17.2	57.3	15.3	51.0
10/90	3.8	38.0	2.7	27.0

As TPU incorporation increased in the formulation, overall percent crystallinity decreased. There is minimal change in the PLA fraction crystallinity from melting until 30/70 which showed an increase in crystallinity that was greater than that of 100% PLA filament. The same trend was observed for PLA fraction crystallinity from

recrystallization. At 10/90 there is a substantial decrease in PLA fraction crystallinity which suggests that at high TPU incorporation, PLA crystallinity is hindered by significant separation of PLA chains by the TPU matrix to the point that crystallinity is significantly decreased.⁶⁷

5.7 Melt Flow Indexing of Twin-screw Filament Blends

Melt flow indexing was performed on twin-screw filament blends to characterize rheological properties of the blends. Table 27 displays the average melt values of twin-screw filament blends. The values are an average of three specimens per sample with standard deviation.

Table 27. Melt Flow Index Values for Twin-screw Extrusion

Formulation (%PLA/%TPU)	Melt Flow Index (g/10 min)
Literature Value PLA	9-15
Virgin PLA	16.1 (± 1.1)
Single-screw PLA	14.8 (± 1.2)
Twin-screw PLA	13.4 (± 0.8)
90/10	18.1 (± 1.2)
70/30	17.7 (± 1.9)
50/50	25.5 (± 0.2)
30/70	43.6 (± 4.4)
10/90	48.3 (± 4.9)
0/100	38.3 (± 8.1)
Literature Value TPU	20-60

As concentrations of TPU were incorporated into the filament blends, a steady increase in melt flow index value was observed. The higher melt flow index indicated a reduced resistance to flow as more TPU was incorporated into the blends. Blend viscosity decreased and became predominated by the high MFI TPU rather than the lower MFI PLA as TPU incorporation increased, allowing for higher overall melt flow. Lower melt viscosity among TPU blends allows PLA chains to move more freely in the melt and may

explain why PLA faction crystallinity increases with higher concentrations of TPU up to a certain blend composition.⁶⁸

5.8 Tensile Testing of Twin-screw Filament Blends

Tensile testing was performed on twin-screw filaments to characterize mechanical properties. Table 28 displays the average tensile values of optimized filament blends. The values are an average of ten specimens per sample with standard deviation.

Table 28. Tensile Modulus and Ultimate Elongation of Twin-screw Filament

Formulation (%PLA/%TPU)	Modulus (Mpa)	Ultimate Elongation (%)
100/0	4911 (± 340)	2 (± 0.3)
90/10	4677 (± 475)	2 (± 0.3)
70/30	3214 (± 359)	1.2 (± 0.1)
50/50	2078 (± 454)	87 (± 10)
30/70	756 (± 234)	109 (± 6)
10/90	8 (± 0.9)	131 (± 14)
0/100	3 (± 0.5)	155 (± 23)

As TPU concentration increased within a blend, filament modulus decreased. Elongation followed an inverse trend with the increase in TPU; elongation increased as the concentration of TPU increased. As TPU concentrations increased, so did the overall elastomeric character of the material provided by soft segments of TPU. This attributed to an increase of material flexibility and decrease in material rigidity.⁶⁴

5.9 SEM Characterization of Twin-Screw Blends

SEM was performed on twin-screw filament blends to observe the effective distribution of TPU within the PLA filament matrix. Figure 38 displays the SEM micrographs of optimized filaments.

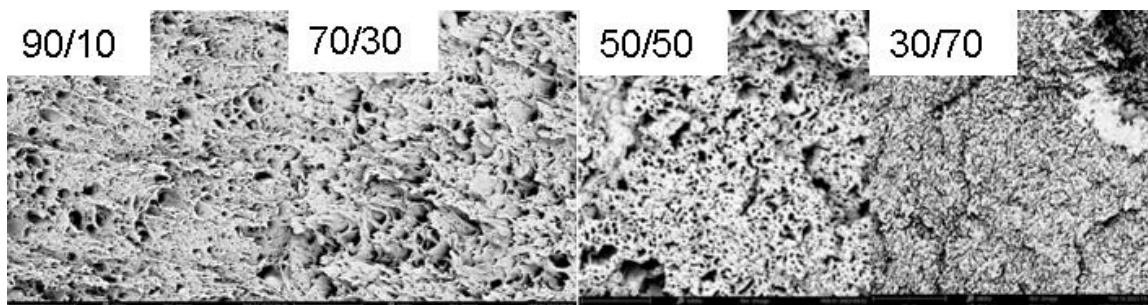


Figure 38. SEM micrographs of twin-screw blends at approximately 6000x magnification.

Table 29 shows the TPU domain size of the optimized filaments measured from the SEM micrographs. As the ratio of TPU within a blend increased, the size of the TPU domains decreased and the number of the TPU domains increased. This change in domain size and quantity is shown in table 29.

Table 29. Domain Size of TPU Domains in Twin-screw Filaments

Formulation (%PLA/%TPU)	Domain Size (nm)
90/10	985 (± 202)
70/30	901 (± 209)
50/50	844 (± 223)
30/70	454 (± 98)

5.10 Injection Molding of PLA/TPU Blends

The different blends ratios were evaluated in comparison to their single-screw and twin-screw counterparts. The Arburg allrounder industrial scale injection molder was used to process all materials evaluated in this work. All test bars and impact samples were molded at optimal parameters.^{11,18} These parameters were determined by the values specified on the material data sheets.^{11,18} To ensure quality data was obtained during subsequent analysis, all molded samples were examined for defects. All injection-molded materials processed on the Arburg and were subject to further testing and analysis. The molded test bars underwent characterization by TGA, DSC, tensile testing, and Izod impact testing. Thermal analysis was performed on the molded test bars by TGA and DSC to investigate the effects of injection molding on PLA/TPU blends. Mechanical

analysis was performed on injection-molded samples by tensile testing and Izod impact testing.

5.11 Appearance of Injection-molded PLA/TPU Blends

Figure 39 shows the appearance of injection-molded PLA/TPU blend samples. Blends consisting of solely PLA appeared to be white in color. As TPU was incorporated into the blends, the test bars appeared to become more yellow, with the most significant visual difference shown in blend 30/70.



Figure 39. Appearance of virgin PLA, single-screw PLA, twin-screw PLA, twin-screw 70/30, twin-screw 30/70, and twin-screw 0/100 injection-molded test bars.

5.12 Thermogravimetric Analysis of Injection-molded PLA/TPU Blends

The thermal stability of injection-molded samples was investigated by TGA. Figure 40 displays the TGA thermograms of the injection-molded samples. The thermal properties of injection-molded samples are summarized in table 30.

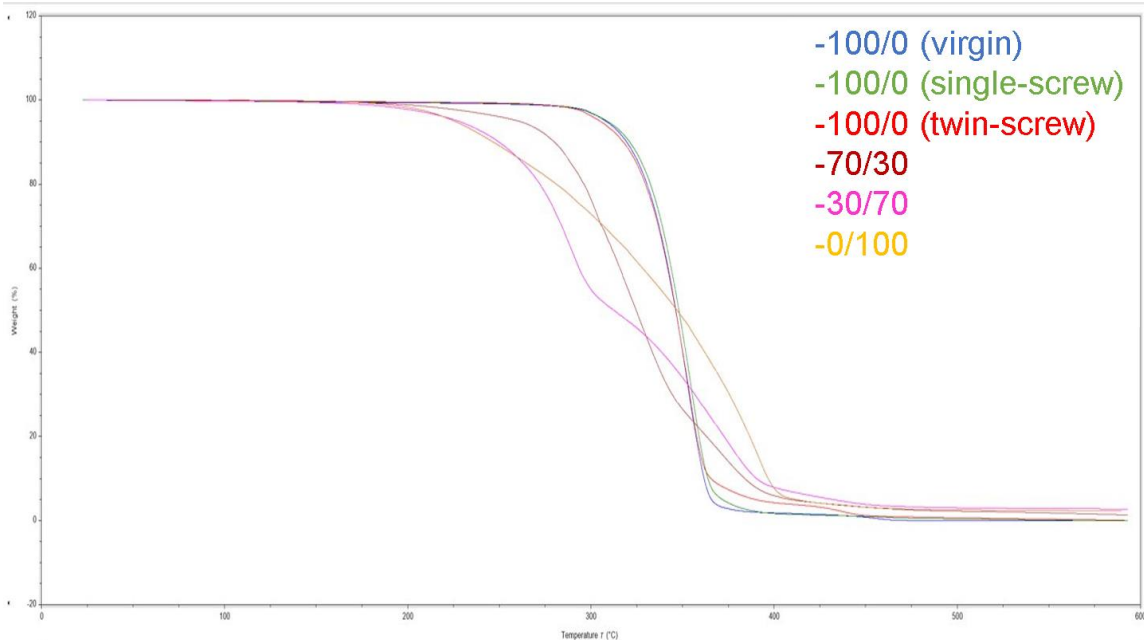


Figure 40. TGA thermograms of injection-molded PLA/TPU test bars: 100/0 (virgin) (—), 100/0 (single-screw) (—), 100/0 (twin-screw) (—), 70/30 (—), 30/70 (—), and 0/100 (—).

Table 30. Thermal Properties as Determined by TGA of Injection-molded Samples

Formulation (%PLA/%TPU)	Temperature @ 10% Weight Loss (°C)	Temperature @ 50% Weight Loss (°C)	Percent Residue (%)
Virgin PLA IJ	319	346	0.0
100/0 IJ (single-screw)	321	348	0.0
100/0 IJ (twin-screw)	317	346	0.0
70/30 IJ	280	324	1.32
30/70 IJ	250	312	2.70
0/100 IJ	247	347	2.28

As values of TPU increase within a blend, a clear decrease in thermal stability was observed at 10% weight loss. The trend is similar at 50% weight loss. As TPU content increases, the rate of decomposition decreased, as demonstrated by the larger differences between 10% weight loss and 50% weight loss as TPU content increased.

5.13 Differential Scanning Calorimetry of Injection-molded PLA/TPU Blends

The thermal behavior of injection-molded samples was investigated by DSC.

Table 31 displays the thermal values for injection-molded samples.

Table 31. Thermal Properties as Determined by DSC of Injection-molded Samples

Formulation (%PLA/%TPU)	T _{g1} (°C)	T _{g2} (°C)	T _c (°C)	T _{m1} (°C)	T _{m2} (°C)	T _{m3} (°C)
Virgin PLA IJ	63	-----	114	144	171	177
100/0 IJ (single-screw)	62	-----	114	144	171	177
100/0 IJ (twin-screw)	62	-----	113	143	170	176
70/30 IJ	-43	46	102	129	161	171
30/70 IJ	-42	-----	87	131	159	-----
0/100 IJ	-46	-----	77	142	160	-----

As concentrations of TPU increased within a filament, a clear decrease in T_g was observed. As more TPU is incorporated within the blends, a second T_g appears on the DSC curve of 70/30. This second T_g shows in polymer systems which are immiscible. The presence of two glass transition temperature indicates a lack of mixing at a molecular level to a certain degree.⁶⁵ T_c also shows a clear decrease in value as TPU content increased. T_m also followed a similar trend. The decrease in thermal transition values can be attributed to a few factors. Greater concentrations of TPU within the system contribute to an overall decrease in thermal stability due to TPU being an amorphous polymer for similar reasons as those discussed in single-screw extruded and twin-screw extruded filaments.⁶⁹

Percent crystallinity was calculated for material samples by dividing the heat of melting or heat of re-crystallization by heat of fusion for their base polymer. The heat of melting and heat of re-crystallization was determined from DSC curves obtained from the polymers.⁵⁹ Crystallinity of the PLA fraction was calculated by dividing the overall crystallinity value by the weight percentage of PLA in the blend.

Table 32. Percent Crystallinity of Injection-molded Samples

Formulation (%PLA/%TPU)	Overall Crystallinity from Melting (%)	PLA Fraction Crystallinity Fraction from Melting (%)	Overall Crystallinity from Recrystallization (%)	PLA Fraction Crystallinity Fraction from Recrystallization (%)
Virgin PLA IJ	38.4	38.4	32.1	32.1
100/0 IJ (single-screw)	47.4	47.4	41.2	41.2
100/0 IJ (twin-screw)	51.0	51.0	43.7	43.7
70/30 IJ	30.8	44.0	30.1	43.0
30/70 IJ	9.8	32.6	9.6	32.0

Percent crystallinity in injection-molded samples differed slightly in pure PLA samples. Injection-molded virgin PLA exhibited an overall melt crystallinity of 38.4%. This was roughly 9% lower than PLA processed from single-screw pellets and 11% lower than PLA processed from twin-screw pellets. Overall crystallinity decreased substantially in 70/30 and 30/70.

5.14 Tensile Testing of Injection-molded PLA/TPU Blends

Tensile testing was performed injection-molded samples to characterize mechanical properties. Table 33 displays the average tensile values of samples. The values are an average of ten specimens per sample with standard deviation.

Table 33. Tensile Modulus and Ultimate Elongation of Injection-molded Samples

Formulation (%PLA/%TPU)	Modulus (Mpa)	Ultimate Elongation (%)
Virgin PLA IJ	2243 (\pm 204)	3 (\pm 0.3)
100/0 IJ (single-screw)	2255(\pm 41)	3 (\pm 0.1)
100/0 IJ (twin-screw)	2286(\pm 49)	3 (\pm 0.1)
70/30 IJ	1564 (\pm 91)	244 (\pm 113)
30/70 IJ	236 (\pm 30)	738 (\pm 16)
0/100 IJ	7 (\pm 0.26)	469 (\pm 60)

There are minimal differences in the modulus and ultimate elongation in the PLA injection-molded samples, indicating that different initial processing has minimal effect on the tensile properties of injection-molded PLA. When TPU was incorporated into the system, filament modulus decreased and ultimate elongation increased with increasing

TPU. This occurred because of the increased TPU incorporation that attributed to an increase of material flexibility and decrease in material rigidity.⁶⁴

5.15 Izod Impact Testing of Injection-molded PLA/TPU Blends

Izod impact testing was performed on injection-molded samples to further characterize mechanical properties. Table 34 displays the average Izod values of injection-molded test bars. The values are an average of ten samples with standard deviation. For each material, half of the samples were left unnotched and the remaining half were notched to test for notch sensitivity. The break type is also noted.

Table 34. Izod Values of Injection-molded PLA/TPU Blends

Formulation (%PLA/%TPU)	Notched	Impact (ft-lb/in)	Break Type
Virgin PLA	No	13.8 (± 2.3)	Hinge
	Yes	1.2 (± 0.3)	Complete
100/0 (Twin-screw)	No	8.8 (± 1.5)	Hinge
	Yes	0.85 (± 0.1)	Complete
100/0 (Single-screw)	No	9.2 (± 1.0)	Hinge
	Yes	0.82 (± 0.1)	Complete
70/30	No	39.99 (± 4.2)	Hinge
	Yes	8.2 (± 0.5)	No break
30/70	No	9.5 (± 2.1)	No break
	Yes	7.7 (± 0.7)	No break
0/100	No	1.9 (± 0.5)	No break
	Yes	1.6 (± 0.7)	No break

As shown in table 34, PLA blends are significantly affected by notch sensitivity. PLA samples processed by single- and twin-screw extrusion showed reduced impact properties compared to virgin PLA. In pure PLA blends, hinge and complete breaks were observed. As TPU was incorporated into the system, impact values decreased except in the notched value of 70/30 which increased substantially. Blends increasing containing TPU did not break, which suggests that TPU incorporation increases material toughness with a beneficial contribution to impact properties.⁷⁰

5.16 3D Printing with PLA Filament

3D printing trials were attempted utilizing the 100/0 twin-screw filament in the Creality Ender 3 Max 3D printer. Figure 41 below details the proposed part and the result of 3D printing.



Figure 41. Proposed 3D printed part design (left) and actual printed part made with 100/0 PLA filament processed by twin-screw extrusion (right).

The complete part could not be successfully printed to completion. The 100/0 PLA filament caused a material feed issue with the feed throat of the 3D printer and a complete part was not able to be successfully printed as a result. It was determined that the 100/0 filament diameter varied too greatly along the length of the filament for the 3D printer to consistently feed successfully, so the processing parameters must be further optimized within dimensional specifications to obtain more consistent filament diameter over many feet.

5.17 Summary

PLA/TPU blends were successfully processed using the LabTech twin-screw extruder. Filament diameter measurement showed that twin-screw extrusion has a significant improvement on cylindricality of filament blends compared to blends processed by single-screw extrusion. Thermal characterization by TGA and DSC showed that thermal stability of PLA/TPU blends decreased as increasing amounts of TPU was

incorporated. Thermal analysis of twin-screw filament blends by DSC showed glass transition temperatures that decreased with the incorporation of TPU. Only two filament blends exhibited two glass transition temperatures: 70/30 and 50/50. These second glass transition temperature values are lower than the value of virgin PLA, suggesting that partial miscibility was accomplished in these blends. The remainder of the twin-screw blends exhibited only a single-glass transition temperature. Crystallization temperatures steadily decreased with TPU incorporation. Melt temperatures exhibited a decrease in temperature with TPU incorporation, with specific blends not exhibiting multiple melt transitions, suggesting that TPU has an effect on the presence of PLA melting transitions.

Percent crystallinity analysis of twin-screw PLA/TPU blends showed a steady decrease in overall crystallinity from melting and recrystallization. PLA fraction crystallinity showed a slight decrease from 100/0 to 90/10. It showed minimal differences until 30/70, where it increased by roughly 8%. It decreased sharply upon reaching 10/90. Mechanical characterization by tensile testing showed that blends modulus decreased steadily as TPU was incorporated into the system. Characterization by SEM showed a decrease in domain size but increase in domain quantity as increasing amounts of TPU were incorporated.

PLA/TPU blends were successfully processed using the Arburg injection molder. Injection molded PLA/TPU blends samples varied in appearance as TPU was incorporated, becoming more yellow with greater TPU incorporation. Thermal characterization by TGA displayed that there were minimal variations between PLA variants. As TPU incorporation increased blend thermal stability decreased and rate of degradation decreased, similar to the trend observed in single- and twin-screw

extruded filament. Thermal characterization by DSC displayed minimal differences between injection molded PLA variants. TPU incorporation into the injection blends decreased glass transition temperatures. With TPU incorporation, a second glass transition temperature appeared at blend 70/30, which is indicative of an immiscible polymer systems. Crystallization temperatures decreased as TPU was incorporated into the injection blends. Melt temperature of injection-molded blends decreased with TPU incorporation. Among injection blends, there are minimal differences in the second and third melt temperatures. Percent crystallinity of injection-molded samples blends displayed a decrease in overall crystallinity from melting following 100/0 IJ as TPU was incorporated. PLA fraction crystallinity from melting and recrystallization also decreased from this point as TPU was incorporated.

Mechanical characterization by tensile testing displayed minimal differences in material moduli between the injection molded PLA variants. TPU incorporation reduced moduli and increased ultimate elongation percentages. Mechanical characterization by Izod impact testing exhibited slight differences in injection molded PLA variants. Injection-molded PLA/TPU blends exhibited a decrease in impact values with TPU incorporation in both notched and un-notched samples with breakage decreasing with increasing TPU incorporation.

CHAPTER VI

6. CONCLUSIONS

6.1 Overview

PLA/TPU blends were successfully processed using three typical plastic processing methods: single-screw extrusion, twin-screw extrusion, and injection molding. The blends were formed into filament by extrusion and molded samples by injection molding to evaluate material properties. Thermal analysis was performed on material pellets, single-screw filament, twin-screw filament, and injection-molded samples by TGA and DSC. TGA was used to evaluate degradation temperatures, thermal stability, and percent residue. DSC was used to evaluate the thermal transition behavior of all blends. Mechanical characterization was performed by tensile testing for single-screw extruded filament, twin-screw extruded filament, and injection molded samples. Izod impact testing was performed for injection-molded samples. Rheological characterization was performed on pellet blends by melt flow index indexing. Morphology of filament blends was determined by SEM.

6.2 PLA Processing

PLA was processed using three different methods: single-screw extrusion, twin-screw extrusion, and injection molding, to determine the effect of processing on material properties. After processing, PLA variants were measured and subjected to various types

of analysis. Single-screw PLA filament was not within the desired specifications of 1.75 mm (± 0.05) in the 0° and 90° direction. Twin-screw PLA filament was within specifications and was closer to a cylindrical profile than single-screw PLA filament. This is due to a greater stability of melt pressure during twin-screw extrusion versus single-screw extrusion.

Thermal analysis was performed by TGA and DSC. Both TGA and DSC analysis of PLA variants showed minimal differences between PLA processed by different methods in regard to degradation and thermal transition properties. Analysis of percent crystallinity of PLA variants showed differences among material generations. Single-screw PLA filament pellet had the lowest percent crystallinity from melting at 45.1%, while twin-screw PLA filament had the highest percent crystallinity from melting at 57%. All other PLA variants had crystallinity from melting between these values. When crystallinity from recrystallization was examined, the overall difference between the highest percent crystallinity (twin-screw PLA filament: 51.2%) and the lowest percent crystallinity (single-screw PLA filament pellet: 40.5%) was similar to that of crystallinity from melting both in magnitude and trend. No clear effect on percent crystallinity was determined based on degree of processing of PLA.

Mechanical analysis of PLA variants showed minimal differences in the moduli between single-screw and twin-screw filament. The modulus of injection-molded PLA variants was slightly lower due to differences in sample geometry between an injection-molded test bar and an extruded filament. PLA rheological analysis showed minimal differences in the melt flow index values among the processing methods to which PLA was subjected. From the thermal, mechanical, and rheological analysis, it was determined

that material processing methods do not have a significant effect on the material properties we studied for PLA. Extrusion method did affect the filament geometry, with twin-screw extrusion producing filament that was within specifications and cylindrical in profile with greater reliability.

6.3 Single-screw Extrusion Versus Twin-screw Extrusion

PLA/TPU blends were successfully extruded using single-screw extrusion and twin-screw extrusion. The blends were molded into filament and then subjected to analysis by diameter measurements, TGA, DSC, tensile testing, and melt flow index rheology. Diameter measurement of single-screw and twin-screw extrusion showed that a majority of blends did not meet the desired specifications. Single-screw blends with increasing amounts of PLA significantly departed significantly from a cylindrical profile. The cylindrical profile improved as more TPU was incorporated. In single-screw extrusion, formulation 100/0 was the furthest away from circularity with a 0° diameter of 1.78 mm and a 90° diameter of 1.90 mm. As TPU was incorporated into the formulations, the circularity between 0° and 90° improved but was still did not meet the specification requirements. The variation of cylindricality with the single-screw filament blends was due to inconsistent melt pressure from the extruder. This problem is commonly known as “extruder surging” i.e., the instability of melt pressure and flow rate at the discharge end of an extruder.⁷¹ This variation in melt pressure caused the filament blends to become oblong. This surging effect can be improved by lowering extruder screw speed, but this may be undesirable in some situations. Since PLA is a rigid polymer, the blends experiencing extruder surging would solidify in the oblong shape. Blends increasing in TPU had better circularity even with inconsistent melt pressure. Because TPU is an

elastic polymer with greater flexibility, during the transition from the melt to solid filament, high TPU-content blends can move closer to a cylindrical profile after undergoing stress inside the extruder.

Twin-screw blends exhibited lower standard deviation values in the 0° and 90° directions than single-screw blends. This demonstrates that twin-screw extrusion was more effective than single-screw extrusion in producing PLA/TPU blends with consistent cylindrical geometry. The following twin-screw blends did not reach the required specification of 1.75 mm (± 0.05): 90/10, 70/30, 50/50, and 10/90. The following blends were within specifications: 100/0, 30/70, and 0/100. These blends did exhibit profiles that were more cylindrical than single-screw extruded blends. With the correct extrusion parameter adjustments, these blends can reach the required dimensional specifications. The lower standard deviations values in the 0° and 90° directions present in the twin-screw blends was due to the absence of “extruder surging” that was present in single-screw extrusion. Twin-screw extruders avoid this effect because they are manufactured to handle much higher screw speeds and shear rates than twin-screw extruders.⁷²

Thermal analysis by TGA of single-screw and twin-screw extruded of PLA/TPU filament showed a steady decrease in thermal stability with increasing TPU incorporation. Blend 100/0 in single-screw extrusion began the onset of degradation at 318 °C with a high rate of degradation, reaching 50% degradation at 349 °C. Blend 100/0 produced by twin-screw extrusion demonstrated thermal values within 4 °C of single-screw extruded PLA filament. As more TPU was incorporated into the systems, the rate of degradation of the blends decreased. This is highly evident by blend 10/90 produced by single-screw and twin-screw extrusion. In the 10/90 blend produced by single-screw

extrusion, onset of degradation began at 242 °C, much lower than the 100/0 blend. Blend 10/90 reached 50% degradation at 345 °C, roughly the same temperature as blend 100/0. A similar trend was present in twin-screw extrusion. These thermal values show that blends with a higher PLA concentration are more thermally stable until the onset of degradation since those values were much higher than high TPU blends. The thermal behavior also demonstrates that TPU incorporation slows the rate of degradation as indicated by the larger difference in temperature values between 10% and 50% weight loss. This variation is due to the difference in polymer morphology between PLA and TPU. The onset of degradation of TPU-dominant blends decreased opposed to PLA-dominant blends due to TPU being an amorphous polymer. The molecular arrangement of amorphous polymers is the cause for the lower onset of degradation. Amorphous polymers are isotropic in flow due to their randomized molecular arrangement, as opposed to semi-crystalline polymer that have crystalline domains in addition to amorphous region. Greater amounts of energy are required to disrupt crystalline domains in addition to the amorphous domains in a semi-crystalline polymer like PLA which is demonstrated by the high onset of degradation temperature in PLA-dominant blends. Less thermal energy is required to melt and subsequently degrade amorphous polymers which is proven by the lower onset degradation values in TPU-dominant blends in both single-screw and twin-screw extrusion.⁷³

Thermal analysis by DSC of single-screw and twin-screw extruded PLA/TPU filament showed a steady decrease in thermal transition values as more TPU was incorporated into the blends. Blend 100/0 (pure PLA) processed by single-screw extrusion and twin-screw extrusion exhibits a glass transition temperature of

approximately 64 °C. Blend 0/100 (pure TPU) processed single-screw extrusion and twin-screw extrusion exhibits a glass transition temperature of approximately -45 °C. In single-screw extrusion, two glass transition temperatures were observed in multiple blends. Because two glass transition temperatures were present in most blends, this showed that the blends were immiscible. Blends 90/10, 70/30, 50/50, and 30/70 showed two glass transition temperatures. In blends 90/10 and 70/30, the second glass transition temperature values were approximately 15 °C lower than that of virgin PLA. This suggests that a small amount of partial miscibility was accomplished in these blends. Melt temperatures and crystallization in single-screw blends decreased with TPU incorporation.

In twin-screw extrusion, two glass transition temperatures were also observed in selected blends: 70/30 and 50/50. In these blends, the second glass transition temperatures were also observed to be much lower than the glass transition temperature of virgin PLA. The second glass transition value of blend 50/50 was approximately 12 °C lower than the second glass transition values of single-screw 90/10 and 70/30. This decrease in glass transition temperature suggests that twin-screw extrusion allows for a greater degree of partial miscibility than single-screw extrusion in PLA/TPU blends because the second glass transition value of 50/50 is closer to being a combination of the glass transition values of virgin PLA and TPU. Melt temperatures in twin-screw extruded blends also decreased with TPU incorporation, but a number of melting transitions were absent in blends compared to single-screw extrusion. In twin-screw blend 50/50, further levels of partial immiscibility were supported by the absence of a melting transition that is present in single-screw blend 50/50.

The presence or absence of distinct glass transition values in samples processed by different types of extrusion is attributed to polymer miscibility, or lack thereof.⁷⁴ Miscible polymers will display a unique glass transition temperature that is a combination of the polymers in the blend. Immiscible polymers will display each glass transition temperature of the components present within the blend.⁷⁴ Partial miscibility in polymers indicates that a part of one polymer component molecularly dissolves in the other polymer component and vice versa while another portion of the polymer is phase separated.⁷⁵ This combination of polymers shifts the glass transition temperature of one polymer to an intermediate value of the virgin material glass transition temperatures, evident in twin-screw blends 70/30 and 50/50. Vigorous mixing, like the mixing experienced by extruded polymers in the melt, may force a greater degree of mixing than molten polymers not subjected to shearing force. The glass transition(s) observed in the blends are indicative of the degree of mixing experienced by the blend components. For example, in single-screw extrusion, 90/10 exhibits two distinct glass transition temperatures at -43.46 °C and 47.94, while blend 90/10 processed by twin-screw extrusion exhibits a single glass transition temperature of 58 °C. The temperature 58 °C is between the value of pure PLA (64 °C) and pure TPU (-45 °C).

The decrease in T_g of the twin-screw 90/10 blend, compared to pure PLA, in combination with the absence of a second T_g contributed by TPU supports evidence of greater mixing in blends processed by twin-screw extrusion, and achievement of a higher level of polymer miscibility in twin-screw extruded blends. Since a single T_g was observed in twin-screw extruded blends, PLA and TPU can be considered partially miscible in these blends. This means that vigorous mixing can force some degree of

miscibility in specific polymer blends, usually in concentrations where one polymer predominates, as indicated by the single glass transition temperature observed in 90/10 and 10/90 blends extruded by twin-screw extrusion. Multiple blends processed by twin-screw extrusion (90/10, 30/70, and 10/90) exhibited only a single glass transition temperature without the use of additional chemical compatibilizers. Their single-screw extruded counterparts demonstrated two T_g s, indicating that twin-screw extrusion is forcing some degree of partial miscibility in these PLA/TPU blends.⁷⁴

In terms of percent crystallinity, there are slight differences between single-screw and twin-screw values. There was a steady decrease in overall crystallinity due to dilution of PLA by TPU in blends with increasing TPU incorporation. PLA fraction crystallinity showed differences between single-screw and twin-screw. In single-screw filament blends, overall crystallinity from melting and recrystallization decreased steadily with TPU incorporation. PLA fraction crystallinity for single-screw blends showed an increase in melt and recrystallization crystallinity with the incorporation of TPU, until blend 30/70 where a decrease is observed. The overall crystallinity value for twin-screw 100/0 is slightly higher than single-screw at 52.2%. For twin-screw blends, PLA fraction crystallinity decreases slightly until 30/70 where it increases, similar to the trend observed with single-screw extruded blends. The increases in material crystallinity suggests that as TPU ratio increases, PLA is being forced into smaller domains that result in more tightly packed polymer chains, resulting in greater tendency to crystallize in these domains. After a certain point, however, there is not enough PLA in the overall system to sustain a further increase in PLA fraction crystallinity and crystallization is actively being inhibited by TPU.

Tensile testing showed a steady decrease in material modulus for both single-screw and twin-screw extruded PLA/TPU filaments as TPU incorporation increased. This decrease was not only entirely expected, but it was one of the main reasons for blending PLA with TPU: increasing flexibility and elongation, while sacrificing some degree of tensile strength. Twin-screw extruded filament modulus values exhibited slightly lower values at higher PLA incorporation than those extruded by single-screw extrusion. Single-screw 100/0 showed a modulus of 5762 MPa (± 1025). Twin-screw 100/0 showed a modulus of 4911 MPa (± 340). Despite this initial difference in moduli, both single-screw and twin-screw moduli decrease similarly until blend 30/70, where there is a sharp decrease. Single-screw 30/70 shows a decrease from 2056 MPa (± 169) to 18.5 MPa (± 2.2). Twin-screw 30/70 also shows this reduction, albeit more less severe. Twin-screw 50/50 reported a modulus of 2078 MPa (± 454) and 30/70 reported a modulus of 756 MPa (± 234). Twin-screw filament modulus values exhibited narrower standard deviations. The tighter standard deviation values indicate that the tensile moduli of twin-screw blends were more consistent over the number of samples tested compared to single-screw blends.

SEM analysis of single-screw and twin-screw filaments showed a substantial difference in the domain sizes in the case of all samples analyzed by SEM. Overall, TPU domains were smaller in twin-screw extruded filament than in the corresponding single-screw filament blend. In the 90/10 blend, twin-screw domains were approximately 205 nm smaller than single-screw 90/10 domains. In the 70/30 blend, twin-screw domains were approximately 400 nm smaller than single-screw 70/30 domains. In the 50/50 blend, twin-screw domains were approximately 200 nm smaller than single-screw domains. In

the 30/70 blend, twin-screw domains were approximately 450 nm smaller than single-screw domains.

The smaller TPU domain sizes with a larger overall number of TPU domains observed in twin-screw extruded filament is attributed to a superior level of mixing in the twin-screw extruder. In a co-rotating twin-screw extruder, the very small gap between the screws, or the meshing zone, subjects molten plastic to high shear rates and shearing forces. The result is a mixing effect is much greater than that of a single-screw extruder. Single-screw extruders can also mix molten polymers, as demonstrated by the dispersion of TPU domains in single-screw extruded filaments, but their mechanism of mixing is different. Single-screw extruders mix through dispersive and distributive mixing. Dispersive mixing is like putting two materials to be mixed between two plates and rotating one of the plates. The shear stress developed between the plates would be proportional to the distance between the plates and the speed at which the plate was rotated. Distributive mixing is like putting the two materials in a bowl and stirring them with a spoon. The number and path of the spoon strokes would be proportional to the degree of mixing. Twin-screw extruders mix through dispersive mixing in kneading blocks, but also mix through extensional mixing in mixing elements on the screws. In twin-screw extruders, extensional mixing is accomplished by molten polymer being pulled and pushed through the channels in the extruder by the co-rotating screws, effecting greater degrees of mixing than in a single-screw extruder.^{75,76}

6.4 Viability of Injection Molding PLA/TPU Blends

PLA/TPU blends were successfully processed by injection molding. The blends were molded into injection molded samples to evaluate material properties. PLA blends were analyzed by TGA, DSC, tensile testing, and Izod impact testing. TGA thermal analysis showed a decrease in thermal stability as more TPU is incorporated, similar to the results observed with filament blends. DSC thermal analysis showed minimal differences in thermal transitions present in PLA injection-molded samples. As TPU was incorporated, effects of increasing TPU on T_g and T_m were similar to those observed in twin-screw extruded filament. Viability of injection molding PLA/TPU blends requires more trials at varying PLA/TPU blends ratios. Blends containing higher concentrations of PLA were able to be successfully injection-molded with minimal error. Once blend ratios increased in TPU, particularly 30/70, parts exhibited issues with mold release. This was likely due to the ejector pins unable to properly eject the higher-TPU blends due to their elastic nature. Further optimization of PLA/TPU blends is warranted as are further injection molding trials of 90/10, 50/50, and 10/90 blends.

6.5 3D Printing

3D printing trials were attempted utilizing the 100/0 twin-screw filament blend, but were ultimately unsuccessful in producing a completed part. The variations along the length of the filament were too great and resulted in a material feed issue with the feed throat of the 3D printer. In order for 3D printing to be successful, greater diameter control will be required over the entire length of the filament.

6.6 Future Work

This project was initiated with the intention to process, identify, and utilize PLA/TPU blended filaments for 3D printing. Minimal 3D printing trials were able to be performed due to issue with filament feeding during printing. Even though the 100/0 blend chosen for 3D printing was had nominally appropriate specifications, variations in the filament diameter and geometry still resulted in improper feeding in the 3D printer. Even the slight inconsistencies in the filament caused the 3D printer to be unable to feed the filament properly. The immediate next project steps are to adjust twin-screw extrusion processing parameters for all filament blends for consistent and within-spec diameters. Once diameter specifications are consistently met, 3D printing trials should occur for each filament blend. After all blends are successfully 3D printed and printing procedures are optimized, 3D printed parts will be analyzed to determine which PLA/TPU filament blend can be printed most successfully.

There were limited injection molding trials with filament blends. The next three blends to utilize for injection molding are 90/10, 50/50, and 10/90 to see how they compare to previously processed blends. Observation of the different properties of each blend ratio should be observed through thermal, mechanical, and morphological analysis similar to that performed on previously injection-molded PLA/TPU blends.

6.7 Summary

In summary, PLA/TPU blends were successfully processed using three typical plastics processing methods: single-screw extrusion, twin-screw extrusion, and injection molding. PLA was investigated to see if different processing methods had an effect on material properties. PLA processing investigations were performed on single-screw,

twin-screw, and injection-molded PLA variants. These variants were subjected to characterization and analysis after processing. Thermal analysis by DSC and TGA shows minimal differences between material generation in regard to thermal and transitional properties. Analysis of percent crystallinity of PLA variants showed slight differences among material generations, likely due to crystallinity increases from chain scission due to mechanical shearing. Despite the differences, percent crystallinity had little effect on mechanical properties. It was determined that processing methods do not have a significant effect on material properties.

PLA/TPU blends were successfully extruded using single-screw and twin-screw extrusion. The blends were molded into filament and then subjected to the respective analysis. Diameter measurements shows differences between single-screw and twin-screw blends, with a majority of blends not meeting the required diameter specification of 1.75 mm (± 0.05). Twin-screw blends exhibited more of a cylindrical profile than single-screw blends. The variation in cylindricality in single-screw extrusion was attributed to “extruder surging”, which is the instability of melt pressure and flow rate at the discharge end of the extruder. Twin-screw blends did not have this issue due to consistencies in melt pressure. Twin-screw blends exhibited lower standard deviation values than single-screw blends. This demonstrates that twin-screw extrusion was more effective than single-screw extrusion in producing PLA/TPU blends with consistent cylindrical geometry.

Thermal analysis by TGA in both single-screw and twin-screw filament blends shows that blends with a higher concentration of PLA were more thermally stable. The thermal behavior also demonstrates that TPU incorporation slows the rate of degradation

as indicated by the larger difference in temperature values between 10% and 50% weight loss. This was attributed to differences in polymer morphology between amorphous TPU and semi-crystalline PLA. Thermal analysis by DSC showed differences in glass transition temperatures in filament blends processed by different methods, which was attributed to polymer miscibility. The differences in glass transitions in single-screw versus twin-screw filament blends was attributed to twin-screw extrusion accomplishing a higher level of polymer miscibility through mixing than single-screw blends. Percent crystallinity showed differences between single-screw and twin-screw filament blends. Differences in crystallinity based on blend ratio suggest that PLA crystallinity increases as TPU is incorporated due to tighter packing of PLA crystals from the TPU domains. SEM analysis showed that twin-screw extrusion was more successful at mixing on a molecular level than single-screw extrusion, due to smaller domain sizes and lower standard deviation values for those domains.

Injection molding trials demonstrated viability in PLA dominant blends but warrants further trials to investigate further blends ratios: 90/10, 50/50, and 10/90. Further injection molding trials are warranted to see how they compare to previously processed blends. 3D printing trials were attempted with twin-screw filament, and it was determined that filament blends must be further optimized within dimensional specifications. Future work involves further optimization of twin-screw extrusion process parameters followed by 3D printing trials.

REFERENCES

1. What is 3D printer filament? <https://www.raise3d.com/academy/what-is-3d-printer-filament/> (accessed Apr 9, 2023).
2. Introduction to Extrusion. Dynisco: Franklin, MA, pp 3.
3. Flynt, J. Choosing a filament diameter: 1.75 mm vs. 3.00 mm. <https://3dinsider.com/1-75mm-vs-3-00mm/> (accessed Apr 9, 2023).
4. A comprehensive list of all 3D Printing Technologies (2023). https://manufactur3dmag.com/a-comprehensive-list-of-all-3d-printing-technologies/#Fused_Deposition_Modelling_FDM (accessed Apr 9, 2023).
5. Carolo, L. What is FDM 3D printing? – simply explained. <https://all3dp.com/2/fused-deposition-modeling-fdm-3d-printing-simply-explained/> (accessed Apr 9, 2023).
6. Stone, W. What is the most common material for 3D printing? <https://www.3dprintingspot.com/post/what-is-the-most-common-material-for-3d-printing> (accessed Apr 9, 2023).
7. Joseph, T. M.; Kallingal, A.; Suresh, A. M.; Mahapatra, D. K.; Hasanin, M. S.; Haponiuk, J.; Thomas, S. 3D Printing of Polylactic Acid: Recent Advances and Opportunities. *The International Journal of Advanced Manufacturing Technology* **2023**, *125* (3-4), 1015–1035.
8. What is PLA? (everything you need to know). <https://www.twi-global.com/technical-knowledge/faqs/what-is-pla> (accessed Apr 9, 2023).
9. Ramezani Dana, H.; Ebrahimi, F. Synthesis, Properties, and Applications of Polylactic Acid-Based Polymers. *Polymer Engineering & Science* **2022**, *63* (1), 22–43.

10. National Center for Biotechnology Information. PubChem Compound Summary for CID 612, Lactic Acid. <https://pubchem.ncbi.nlm.nih.gov/compound/Lactic-Acid>. (accessed April 9, 2023)
11. Ingeo Biopolymer 3D870 Technical Data Sheet. NatureWorks, Minnetonka, MN.
12. Comprehensive guide on Acrylonitrile Butadiene Styrene (ABS). <https://omnexus.specialchem.com/selection-guide/acrylonitrile-butadiene-styrene-abs-plastic> (accessed April 9, 2023).
13. Materials - large scale 3D printing. [https://www.cosineadditive.com/en/materials#:~:text=THERMAL%20EXPANSION\(CTE\)%3A%2068,has%20a%20lower%20melting%20temperature](https://www.cosineadditive.com/en/materials#:~:text=THERMAL%20EXPANSION(CTE)%3A%2068,has%20a%20lower%20melting%20temperature) (accessed April 9, 2023).
14. Heat - thermal expansion: Characteristics of Fine Ceramics: Fine ceramics world. <https://global.kyocera.com/fcworld/charact/heat/thermaexpan.html#:~:text=Low%20Thermal%20Expansion&text=The%20coefficient%20ratio%20of%20thermal,half%20those%20of%20stainless%20steels> (accessed April 9, 2023).
15. Layer separation and splitting. <https://www.simplify3d.com/resources/print-quality-troubleshooting/layer-separation-and-splitting/> (accessed Apr 9, 2023).
16. de Souza, F. M.; Kahol, P. K.; Gupta, R. K. Introduction to Polyurethane Chemistry. *ACS Symposium Series* **2021**, 1–24.
17. Madhusa. Difference between TPU and Pu: Definition, structure, applications, production and differences. <https://pediaa.com/difference-between-tpu-and-pu/> (accessed April 9, 2023).

18. Elastollan[®] TPU Technical Data Sheet. BASF, Florham Park, New Jersey, November 2018.
19. ENGAGE[™] Polyolefin Elastomers. The Dow Chemical Company, Midland, Michigan, 2019.
20. Covestro. Chemical-physical structure: Technology by Covestro.
<https://solutions.covestro.com/en/highlights/articles/theme/product-technology/chemical-physical-structure-tpu> (accessed April 9, 2023).
21. Turney, D. History of 3D printing: It's older than you think.
<https://redshift.autodesk.com/articles/history-of-3d-printing> (accessed Apr 9, 2023).
22. FDM 3D printing - fused deposition modeling. <https://www.stratasys.com/en/guide-to-3d-printing/technologies-and-materials/fdm-technology/> (accessed Apr 9, 2023).
23. Mwema, F. M.; Akinlabi, E. T. Basics of Fused Deposition Modelling (FDM). *Fused Deposition Modeling* **2020**, 1–15.
24. Xometry, T. PLA (polylactic acid): Definition, applications, and different types.
<https://www.xometry.com/resources/materials/what-is-pla/> (accessed April 9, 2023).
25. Miscible polymer blends. <https://pslc.ws/macrog/blend.htm> (accessed April 9, 2023).
26. Millipore Sigma. Solvent Miscibility Table.
<https://www.sigmaaldrich.com/US/en/technical-documents/technical-article/analytical-chemistry/purification/solvent-miscibility-table> (accessed Apr 9, 2023).
27. Guru, GS.; Prasad, P.; Shivakumar, HR.; Rai, SK.; Miscibility , Thermal, and Mechanical Studies of Methylcellulose/Poly(vinyl alcohol) Blends, **2012**. 957-968.

28. Arrighi, V.; Cowie, J. M. G.; Fuhrmann, S.; Youssef, A. Miscibility Criterion in Polymer Blends and Its Determination. *Encyclopedia of Polymer Blends* **2016**, 153–198.
29. Jašo, V.; Cvetinov, M.; Rakić, S.; Petrović, Z. S. Bio-Plastics and Elastomers from Polylactic Acid/Thermoplastic Polyurethane Blends. *Journal of Applied Polymer Science* **2014**, *131*
30. Subramanian, M. N. *Introduction to polymer compounding: Raw Materials*; Smithers Rapra Technology: Shropshire, England, 2014.
31. Amazing information on polymer blends - Kruger 2023.
<https://kruger.industries/polymer-blends/> (accessed April 9, 2023).
32. Geiselman, B. Stackpath - Recycling Today.
<https://www.recyclingtoday.com/article/the-expanding-role-of-compatibilizers/> (accessed April 9, 2023).
33. Muthuraj, R.; Misra, M.; Mohanty, A. K. Biodegradable Compatibilized Polymer Blends for Packaging Applications: A Literature Review. *Journal of Applied Polymer Science* **2017**, *135*
34. Hyvärinen, M.; Jabeen, R.; Kärki, T. The Modelling of Extrusion Processes for Polymers—a Review. *Polymers* **2020**, *12*
35. Frankland, J. How much L/D do you really need?
<https://www.ptonline.com/articles/how-much-ld-do-you-really-need> (accessed Apr 9, 2023).

36. Encyclopedia of Chemical Engineering Equipment. Extruders.
<http://encyclopedia.che.engin.umich.edu/Pages/PolymerProcessing/Extruders/Extruders.html> (accessed April 9, 2023).
37. Shah, A.; Gupta, M. Comparison of the Flow in Co-rotating and Counter-rotating Twin-Screw Extruders. *ANTEC*, **2004**, 443-447.
38. Tangram Technology. Extrusion Definitions. http://www.tangram.co.uk/TI-Polymer-Extrusion_Definitions.html (accessed April 9, 2023).
39. Reiloy Westland Corporation. L/D Ratio. <http://reiloyusa.com/processing-tips/screw-design/ld-ratio/> (accessed on April 9, 2023).
40. Ballistreri, A.; Montaudo, G.; Lenz, R. W. Mass Spectral Characterization and Thermal Decomposition Mechanism of Alternating Silarylene-Siloxane Polymers. *Macromolecules*. **1984**, *17*, 1848-1854.
41. Silva, A.; Teixeira, R.; Moutta, R.; Ferreira-Litao, V.; Barros, R. R.; Silva Bon, M. Sugarcane and Woody Biomass Pretreatments for Ethanol Production. *InTech*. **2013**, 47-88.
42. Types of plastic extrusion screw designs. <http://www.thomasnet.com/articles/plastics-rubber/extrusion-screw-design> (accessed April 9, 2023).
43. Polyplastics. What is injection molding?
<https://www.polyplastics.com/en/support/mold/outline/> (accessed April 9, 2023).
44. Banerjee, A. G.; Gupta, S. K. A Step towards Automated Design of Side Actions in Injection Molding of Complex Parts. *Geometric Modeling and Processing - GMP 2006* **2006**, 500–513.

45. Thomasnet. The basics of liquid injection molding.
<http://www.thomasnet.com/about/injection-molded-plastics-60310604.html> (accessed April 9, 2023).
46. Jaycon Systems. Why is injection molding so expensive? <https://medium.com/jaycon-systems/why-is-injection-molding-so-expensive-eda69b6fccb5> (accessed April 10, 2023).
47. Essentra Components. Five Reasons why injection-molded parts are cost-effective.
<https://www.essentracomponents.com/en-us/news/manufacturing/injection-molding/five-reasons-why-injection-molded-parts-are-cost-effective> (accessed April 9, 2023)
48. 3D-Fuel. Does Filament Quality Really Matter?
<https://www.3dfuel.com/blogs/news/does-filament-quality-really-matter#:~:text=Filament%20Diameter&text=Most%203D%20printer%20filament%20comes,referred%20to%20as%203.0mm> (accessed April 9, 2023)
49. Arlington Machinery. Product Detail. <https://www.arlingtonmachinery.com/product-detail/16282/55-ton-arburg-injection-molding-machine-model-320s-500-150-199-oz-made-new-in-1999/> (accessed April 9, 2023).
50. ASTM. Standard Test Methods for Determining the Izod Pendulum Impact Resistance of Plastics. <https://www.astm.org/Standards/D256> (accessed April 9, 2023).
51. ASTM. Standard Test Method for Tensile Properties of Plastics.
<https://www.astm.org/Standards/D638> (accessed April 9, 2023).

52. ASTM. Standard Test Method for Melt Flow Rates of Thermoplastics by Extrusion Plastometer. <https://www.astm.org/Standards/D1238.htm> (accessed April 9, 2023).
53. Research Gate. Tensile Test Specimen. https://www.researchgate.net/figure/The-tensile-test-specimen-ASTM-D638-Type-1-t-32-mm_fig1_320601269 (accessed April 9, 2023).
54. Testing Machines Inc. Product Search. <https://www.testingmachines.com/search> (accessed April 9, 2023).
55. ASTM. Standard Test Methods for Determining the Izod Pendulum Impact Resistance of Plastics. <https://www.astm.org/Standards/D256> (accessed April 9, 2023).
56. Research Gate. Izod Impact Specimen. https://www.researchgate.net/figure/Dimensions-of-an-Izod-impact-specimen_fig1_335276706 (accessed April 9, 2023).
57. CFAM Technologies. Twin-screw Extruder vs. Single-screw Extruder. <https://medium.com/@cfamtechnology/twin-screw-extruder-vs-single-screw-extruder-87e0fd1861d0> (accessed April 10, 2023)
58. Stevens, M. J.; Covas, J. A. Principles of Melt Flow in Single-Screw Extruders. *Extruder Principles and Operation* **1995**, 127–174.
59. Bourbigot, S.; Garnier, L.; Duquesne, F. R. Characterization of the morphology of isotactic polypropylene/syndiotactic polypropylene blends with various compositions. *Polymer Letters*. **2013**, 224-237.

60. Henriques, I. R.; Borges, L. A.; Costa, M. F.; Soares, B. G.; Castello, D. A. Comparisons of Complex Modulus Provided by Different DMA. *Polymer Testing* **2018**, 394–406.
61. Schyns, Z. O.; Shaver, M. P. Mechanical Recycling of Packaging Plastics: A Review. *Macromolecular Rapid Communications* **2020**.
62. Lin, Y.; Bilotti, E.; Bastiaansen, C. W. M.; Peijs, T. Transparent Semi-Crystalline Polymeric Materials and Their Nanocomposites: A Review. *Polymer Engineering & Science* **2020**, 2351–2376.
63. Ashfaq, S. The complete guide shape memory materials and their applications. <https://polymerexpert.fr/en/r-d/the-complete-guide-shape-memory-materials-and-their-applications/> (accessed Apr 25, 2023).
64. Huang, H.; Pang, H.; Huang, J.; Yu, P.; Li, J.; Lu, M.; Liao, B. Influence of Hard Segment Content and Soft Segment Length on the Microphase Structure and Mechanical Performance of Polyurethane-Based Polymer Concrete. *Construction and Building Materials* **2021**
65. Thirtha, V.; Lehman, R.; Nosker, T. Morphological Effects on Glass Transition Behavior in Selected Immiscible Blends of Amorphous and Semicrystalline Polymers. *Polymer* **2006**, 5392–5401.
66. Polymers, M. C. An introduction to amorphous polymers. <https://www.mcpolymers.com/library/introduction-to-amorphous-polymers> (accessed Apr 25, 2023).

67. Arai, F.; Shinohara, K.; Nagasawa, N.; Takeshita, H.; Takenaka, K.; Miya, M.; Shiomi, T. Crystallization Behavior and Higher-Order Structure in Miscible Crystalline/Crystalline Polymer Blends. *Polymer Journal* **2013**, 921–928.
68. Polymer Entanglement. <https://sites.psu.edu/stm9research/research/polymer-entanglement/> (accessed Apr 25, 2023).
69. Advanced EMC Technologies. Amorphous Vs. Semi-crystalline Polymers. [Amorphous vs. Semi-Crystalline Polymers - Advanced EMC Technologies | High Performance Polymer Seals & Bearings \(advanced-emc.com\)](https://www.advanced-emc.com/Amorphous-vs.-Semi-Crystalline-Polymers-Advanced-EMC-Technologies-High-Performance-Polymer-Seals-Bearings-advanced-emc.com) (accessed April 9, 2023)
70. Chang, F.-chih; Yang, M.-Y. Mechanical Fracture Behavior of Polyacetal and Thermoplastic Polyurethane Elastomer Toughened Polyacetal. *Polymer Engineering and Science* **1990**, 543–552.
71. Campbell, G. A.; Spalding, M. A. Flow Surging. *Analyzing and Troubleshooting Single-Screw Extruders* **2020**.
72. Twin Screw Extruder vs Single Screw Extruder. <https://www.cowellextrusion.com/twin-screw-extruder-vs-single-screw-extruder/> (accessed Apr 25, 2023).
73. Santmartí, A.; Lee, K.-Y. Crystallinity and Thermal Stability of Nanocellulose. *Nanocellulose and Sustainability* **2018**, 67–86.
74. Nara, S.; Oyama, H. T. Effects of Partial Miscibility on the Structure and Properties of Novel High Performance Blends Composed of Poly(p-Phenylene Sulfide) and Poly(Phenylsulfone). *Polymer Journal* **2014**, 568–575.

75. Carson, S. O.; Maia, J. M.; Covas, J. A. A New Extensional Mixing Element for Improved Dispersive Mixing in Twin-Screw Extrusion, Part 2: Experimental Validation for Immiscible Polymer Blends. *Advances in Polymer Technology* **2016**, 167–175.

76. Hinch, E. J. Lecture 1: Introduction. *Fluid Mechanic Preliminaries*, 2023.